URANYL COMPLEXES WITH NITROGEN AND SULFUR DONOR BIDENTATE LIGANDS: A COMPUTATIONAL MODELING OF COORDINATION GEOMETRIES, THERMODYNAMIC PARAMETERS, AND LIGAND SUBSTITUENT EFFECTS

A thesis presented to the faculty of the Graduate School of Western Carolina University in partial fulfillment of the requirements for the degree of Masters of Science in Chemistry.

By

Patrick Bailey Hogsed

Advisor: Dr. De Silva
Associate Professor of Chemistry
Department of Chemistry & Physics

Committee Members: Dr. Channa De Silva, Chemistry & Physics
Dr. Brian Dinkelmeyer, Chemistry & Physics
Dr. Scott Huffman, Chemistry & Physics

July 2021

ACKNOWLEDGEMENTS

Firstly, I would like to thank those that are in my everyday life. These are my family and friends that support me daily. Whether giving me the motivation to write this thesis or lending me an ear to vent to, they are consistently at my side. I wouldn't be where I am today without you all.

Secondly, I would like to acknowledge the educators, advisors, and faculty. Through your wisdom and guidance, you've sharpened and honed my skills. This has given me confidence in my ability and will guarantee the decisions I make in the future are positive ones. The education that you've brought me will propagate through the centuries and have a lasting impact.

Lastly, the random acts of kindness and the people that I don't see. If it was something as simple as opening a door for me or something more complex like writing me a letter, these people always managed to restore my faith that there is good in the world. Their gestures always gave me an extra boost of morale and were just what I needed to get the job done.

Funding:

–Western Carolina University Summer Research Grant

–Western Carolina University Hunter Scholar Award

TABLE OF CONTENTS

LIST OF TABLES

LIST OF FIGURES

ABSTRACT

URANYL COMPLEXES WITH NITROGEN AND SULFUR DONOR BIDENTATE LIGANDS: A COMPUTATIONAL MODELING OF COORDINATION GEOMETRIES, THERMODYNAMIC PARAMETERS, AND LIGAND SUBSTITUENT EFFECTS

Patrick Bailey Hogsed, Masters of Science in Chemistry

Western Carolina University (July 2021)

Advisor: Dr. Channa De Silva

Actinides represent a special group of metal ions that need to be extensively studied due to their presence in the environment with the construction of nuclear power plants, processing of minerals, and weapon production. Radioactive waste produced by nuclear fission contains several lanthanide and actinide metals, including uranium. The extraction of uranium from nuclear waste is an active area of research. To this end, numerous sulfur and nitrogen-donor ligands have been studied to assist with the nuclear extraction process. Computational chemistry investigations of actinide complexes will provide important insight into metal-ligand bonding and their thermodynamic properties in order to design effective actinide extracting agents. Current research work is focused on studying the coordination chemistry behavior and reaction energetics of a series of uranyl metal complexes with ethylenediamine, 1,2-ethanedithiol, and cysteamine ligands using density functional theory (DFT). Coordination preferences using nitrogen and sulfur-based chelation were evaluated in the gas phase. Nitrogen donor ethylenediamine ligand produced the lowest reaction Gibbs free energies, and sulfur donor cysteamine ligands had the highest values. Ligand substitution effects on uranyl metal-ligand bonding were studied using four substituent groups, CH_3, CN, OCH_3, and Cl. Electron donor CH_3 and OCH_3 groups provided relatively shorter metal-ligand bond distances and lower reaction Gibbs free energies. Electron withdrawing substituents resulted in longer metal-ligand bonding and higher reaction Gibbs free energies.

Disubstitution of the chelating ligands amplifies the above effects. Future work will focus on exploring more substituents and solvent effects on uranyl metal-ligand complexation reaction using the above ligands

CHAPTER ONE: INTRODUCTION

Background

U.S. Energy Demand and Nuclear Energy Production

Roughly 80% of all energy produced in the United States can be traced back to the combustion of hydrocarbons. Six billion metric tons of CO_2 are emitted annually just from the U.S. alone.[1] Not only is this terrible for the environment and the future of our planet, but it is also not a reliable long-term solution. Currently, 8% of energy comes from nuclear power[2], which produces a negligible amount of carbon emissions compared to traditional hydrocarbon burning. Nuclear power provides all of the energy that conventional hydrocarbons do without worrying about pollutants in our atmosphere. However, nuclear power isn't currently viable because there isn't a cost-effective solution for fast and safe waste recycling. Nuclear power combined with renewable sources, such as solar, could drastically reduce our dependency on fossil fuels.

The energy produced from a nuclear reactor comes from the immense heat created from fission[3]. A two-loop system is used, independently having its water supply. The primary loop starts at the top of the reaction chamber and corkscrews through the secondary loop's water reservoir. The secondary loop's function is to create steam from the heat transported by the primary loop: this steam is then moved to a turbine, spun to create electrical energy. Control rods are used to capture excess neutrons in the system. By manually removing or adding the control rods, we can maintain the speed at which the reaction occurs[3]. This is visually realized in Figure 1.

Nuclear waste isn't safe for any living organism because of its radioactivity. This occurs when there is an unstable isotope present. Isotopes of various elements can be found in nuclear waste: these isotopes are incredibly unstable and emit harmful alpha, beta, and gamma rays[4]. Alpha and beta rays don't penetrate nearly as deeply as gamma rays; because gamma rays are high energy, the only things that can stop them from penetrating are very thick concrete or layers upon layers of material. To prevent these isotopes from interacting with life, getting them as far away as pos-

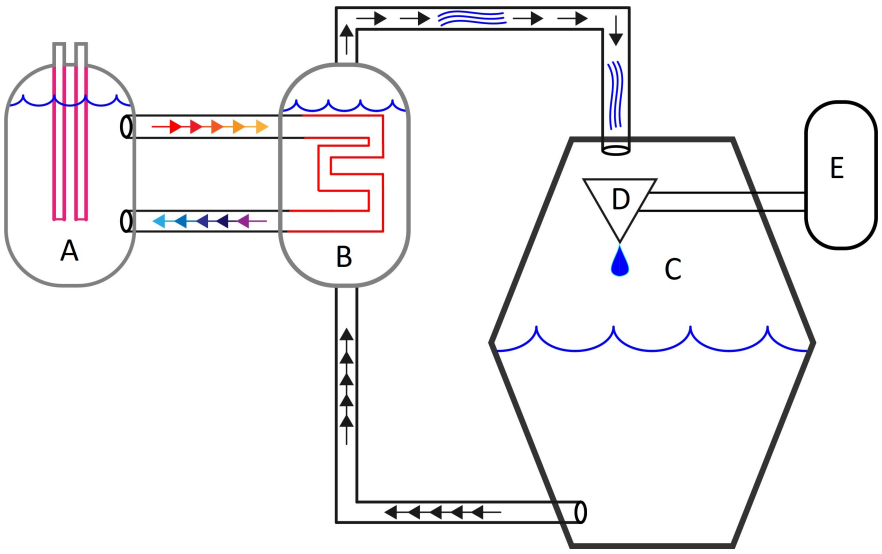

Figure 1. Fundamental schematic of a nuclear reactor. A: nuclear reaction chamber where water is heated. B: water heated through convection and turned to steam. C: steam spins turbine (D), producing energy in E, and condenses into water.

sible is a priority. This means either burying the nuclear waste or sealing it in concrete bunkers[5]. Deep storage units are the current solution for nuclear waste. However, we still aren't aware of the long-term environmental impacts of doing so. This could lead to substantial problems in the future[6], and is one of the main reasons why scientists are searching for an alternate method. Ideally, elements from the waste would be extracted and reused, which would create a cycle[7].

The vast majority of nuclear waste is the same uranium used in the fuel rods: only a small portion is converted into fission products[8]. This is because, during the reaction, neutron capturing isotopes are formed, and eventually, they become so abundant that they bring the reaction to a halt. Elements like xenon and zirconium are some of the most commonly found. 95% of waste is a combination of U-235 and U-238 ($\sim$0.4% and $\sim$94% respectively).[9] The differentiating factor between the two is U-235 is fissile while U-238 is not. The uranium isotopes found in the waste are the same ones found in nuclear fuel rods.

Uranium Species Found in Nature

Typically, uranium is found in one of two states in nature. It's either in a crystalline state or an aqueous state. Species found in an aqueous state can be found having two oxygen atoms attached to the metal center. The only place where this is not the case is at extremely low pH.[10] Because nuclear waste is an aqueous solution, the UO_2^{2+} (Figure 2) model is very relevant. Nuclear waste has a pH ranging from 11.5 to 12.5, and it has an oxidation-reduction potential of a little less than zero; this means that the species we will be working with is UO_2^{2+}. This species of uranium has two common names, uranyl, and uraninite. Uranyl will be used to refer to it from this point on. Uranyl, having a +2 charge, typically acts as a hard acceptor. Its electron cloud is tightly knit, and it is unable to be easily polarized. This makes it perfect for working with nitrogen and sulfur chelators. It has also been proven to be effectively extracted from nuclear waste (aqueous) when bound to a nitrogen ligand[11]. For these reasons, the uranyl species will be a great starting point for our research.

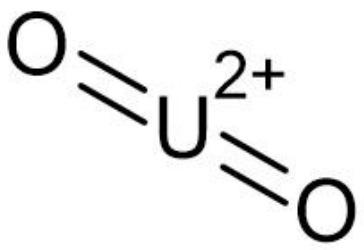

Figure 2. Uranyl (UO_2^{2+})

Importance of La/Ac extraction and current methods

Nuclear waste contains high concentrations of lanthanide and actinide ions, which can be recycled into things like fuel rods, biomedical dyes, and nuclear weapons[12] if adequately extracted. The extraction of these metals seems trivial at first, but the entire process needs to be scaled up

to an industrial scale to keep up with the demand. This means that whatever is used to extract the metal needs to be cheap, environmentally friendly, and abundant. Energy is also something to consider; lower energy processes would mean larger batches could be done.

Methods of transuranic extraction

Bismuth phosphate (Figure 3) is one of the earliest known extractors in the purification of lanthanides and actinides. Plutonium and other lanthanides would precipitate with the bismuth phosphate and leave behind the uranium[13]. This was still in the area where plutonium and other lanthanides were seen as more valuable than their actinide counterparts. So, the uranium that is left behind from the separation was sent to the waste. However, it wasn't pure uranium. Anywhere from 1 to 3% of the waste was plutonium[13]. If the solution was 50% lanthanide's and 50% actinide's, this might not be much of an issue, but 98% of the feed stream was uranium[13]. This led to massive amounts of both uranium and plutonium being wasted.

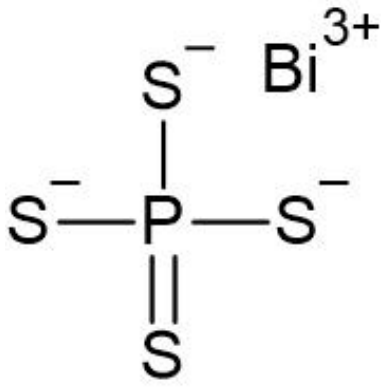

Figure 3. Bismuth Phosphate ($BiPO_4$)

After this loss was realized, efforts were made to better the separation process. Shortly after bismuth phosphate was seen as obsolete, new methods arose, such as Methyl isobutyl ketone (MIBK) and plutonium uranium reduction extraction (PUREX). MIBK oxidized the uranium and

plutonium into a hexavalent state, where it could then undergo additional reactions to purify it further. PUREX is a similar process but uses tributyl phosphate and kerosene instead of MIBK. PUREX has become the standard for purifying nuclear waste into its elemental components. However, this doesn't mean that it's perfect. Its main concern is "proliferation resistance." This is the reduction in worry that the recycling of these elements (P, U, Np...) will lead to an uptick in nuclear weapon manufacturing. Moreover, a system, nuclear power plant, and recycling plant have to become proliferation-resistant in order for them to be seen as viable by the public.

Density Functional Theory (DFT)

Traditionally, calculating a compound's properties can be extremely time-consuming and sometimes inaccurate if done by hand. As an alternative, computational processing promises tremendous power and consistency; it's used in all areas of math and science. In chemistry, it's used for determining the geometrical structure. The geometrical structure of a system gives rise to the properties of that system. Minor changes to the geometry also affect the properties[14], including thermodynamic properties such as free energy and entropy. Isomerization is an excellent example of this. A chemist can then decide whether it is worth pursuing in a physical lab setting by assessing the approximate traits. This saves time and resources that would otherwise be used.

The probability of finding an electron in a space can be calculated by taking the integral of the wave function and its complex conjugate, as seen in Equation 1. ψ is the wave function, and like mathematical waves, it has to be single-valued, continuous, and differentiable. This wave function is like a machine that has input and output. Every eigenvalue that is given as output has to have come from an input operating on the wave function. Due to the conflicting ideas of Heisenberg's uncertainty principle, the wave function had to be reimagined. Max Born had the notion that looking at an electron's exact position is flawed, and instead, it should be thought of as a probability[15].

$$Probability = \int_a^b \psi\psi^* dr \tag{1}$$

We can't talk about computational calculations and ψ without talking about the Schrödinger equation (Equation 2): it will be the time-independent variant for this case. H(t) is the Hamiltonian operator, and it "works" on the wavefunction(ψ). H(t) is the summation of three parts; the kinetic, the potential, and the electron-electron interactions (Equation 3). Some of these terms can be omitted because of the Born-Oppenheimer approximation, which states that the nuclei are moving extremely slow relative to the electrons[15] and allows for the energy to be calculated with stationary nuclei. The variables of this equation are the charge of the particle (Z), r_i is the coordinate of electron i, and R_a is the coordinate of the nucleus with the same charge as Z. Once calculated, there is a correlating eigenvalue (E).

$$H(t)\psi(t) = E\psi(t) \tag{2}$$

$$H(t) = -\frac{1}{2}\sum_{i}^{N}\nabla_i^2 + -\sum_{a}^{N}\frac{Z_a}{|r_i - R_a|} + \sum_{i<j}^{N}\frac{1}{|r_i - r_j|} \tag{3}$$

Now, density functional theory is an improvement upon the all popular Hartree-Fock method (HFM). HFM uses variations of the equations mentioned earlier and an iterative process to calculate ground-state energies of the system[14]. A ground-state stationary point is set (unless convergence fails) for both optimization and frequency calculations[16].

Hohenberg and Kohn were the two pioneers that built upon HFM[17]. Their collective thought was to bring DFT to the world as a viable alternative to the traditional HFM. Together they developed two theorems that would provide a foundation for calculating DFT problems.

Theorem 1. *the ground state of any interacting many-particle system with a given fixed inter-particle interaction is a unique functional of the electron density n(r).*[18]

This boils down to proving that this functional exists, but it doesn't give a solution to it. What it allows for is the ground state energy, E[n(r)], to be written in terms of ground-state density, as

seen in Equation 4[17].

$$E[n(r)] = \int n(r)v_{ext}(r)dr + F[n(r)] \tag{4}$$

Theorem 2. *the ground state energy can be obtained variationally: the density that minimizes the total energy is the exact ground-state density*[17].

This means that by applying variational theory, the electron density can be changed to minimize the energy. Once it has found its minima, the ground state electron density is found, and the properties can be calculated fully[19]. What Hohenberg and Kohn did was very impressive, but it still left work to be done. There needed to be an equation that included the density functional and can be varied without contradicting itself. Kohn and Sham were the first to start working on a new solution for this mystery.

Kohn and Sham supposed that the kinetic energy of a density could be calculated through a single Slater determinant. That is, a wave function would have to have a single Slater determinant and also correspond to an electron density. This is very reminiscent of HFM because it uses Slater determinants to calculate kinetic energy. Together they developed a series of equations that proved their hypothesis (Equations 5-6), except for one piece. The exchange-correlation piece (E_{xc}[r]) is extremely complicated and is still not known. Because of this reason, we use approximations for the exchange correlations, such as B3LYP[8].

$$E_{KS-DFT}[r] = T_s[r] + E_{eN}[r] + J[r] + E_{xc}[r] \tag{5}$$

$$E_{xc}[r] = (T[r] - T_s[r]) + (E_{ee}[r] - J[r]) \tag{6}$$

Methods and Basis sets

There are a series of computational parameters around DFT that allow for every calculation to be specialized according to what needs to be calculated. These are most commonly known as basis sets and methods. Basis sets can be thought of as a culmination of functions that represent the

wave function for a given system. The earliest example we've seen of this is the hydrogen atom being a 1S orbital. The "1S" gives us information about the system, similar to what a basis set would provide during a calculation. Methods are the other part of the calculation: they define how the energy is calculated. In fact, a method was mentioned earlier, "B3LYP."

Basis sets in quantum chemistry are usually seen as the linear combination of atomic orbitals, which gives us a wave function for a molecular orbital (Equation 7). This basically states that the wave function of molecular orbitals is formed from the summation of atomic orbital wave functions. Now, there are several options for basis functions to choose from, and they all have their pros and cons. The main three are Slater type orbitals (STO), Gaussian type orbitals (GTO), and contracted Gaussian type orbitals (CGTO). The basis set can be a spectrum of inclusivity when it comes to these basis functions. It can be as small as including one basis function per atomic orbital, or you can have several basis functions per atomic orbital.

$$\psi_i = \sum_n c_n, i\phi_n \tag{7}$$

Split basis sets are a little different because they only use one basis function for every core atomic orbital and that they use numerous business functions for the outer valence atomic orbitals. As an example, look at 6-311G. 6 refers to the number of GTO functions describing the inner atomic orbital. 3 is the number of GTO functions in the first STO. 1 and 1 are the number of GTO functions in the second and third Slater type orbital, respectively.

B3LYP is actually a hybrid method and is comprised of two parts; B3 is Becke's 3 parameter exchange-correlation functional, and LYP is Lee Yang and Parr correlation functional. B3LYP was created to be a great improvement on HFM. It achieved this status when it was realized that the calculations were faster and yielded comparable results. At this point in time, B3LYP is highly respected and well established. This is one of the benefits of using a well-known method is that calculations will be reliable and unquestioned.

Efective core potentials

Effective core potentials (ECP) replace core electron basis functions and get replaced with an effective potential. This allows for the complexity of the calculation to decrease tremendously and reduces calculation time also. This is especially useful for larger systems with several different atoms. While this ECP is essentially an approximation, it allows for relativistic effects to be calculated. ECPs are commonly used with heavier metals that have an array of different shells.

Previous Computational Research on Uranyl Complexes

Studying the extraction of La and Ac ions from nuclear waste is still a relatively new field. Most of the research done in this area is within the past two decades. The current studies offer a strong indication that nitrogen is the leading element to aid in extraction, specifically monoamide bidentate ligands[11]. Newer articles suggest that sulfur could also be prominent as a ligand or at least play a role as an intermediate in the process. Others are focusing on the properties of the complexes, such as substituent effects.

Sulfur Chelation onto Uranyl

Townsend et al.[20] worked with relevant uranium molecules in environmental conditions similar to those found in nature. The team started with a U(VI) sorbed to ferrihydrite; the uranyl complex was saturated with oxygen atoms. Using computational modeling, they simulated the molecule undergoing sulfidation. Later, they used XAS (X-ray Absorption Spectroscopy) and EXAFS (Extended X-ray Absorption Fine Structures) to confirm that an intermediate was forming. This new molecule was a water-saturated uranyl complex with a persulfide attached to the metal center as seen in Figure 4.

This data also confirmed that the water molecules and that the new persulfide ligand was in the same plane as each other. The UO_2 metal was uninterrupted and remained ”upright.” Townsend and colleagues were curious about the range of complexes that could be achieved using plane-wave density functional theory. They were looking at both isolated molecular species and surface adsorbed models. For the isolated molecular species, their data came back inconsistent with what

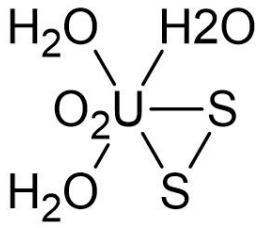

Figure 4. Persulfide intermediate

they had previously seen from EXAFS. They instead tried to inject the persulfide directly into the same plane as the oxygen. This time it worked, and the most stable complex that came back was again the one with three water molecules and the persulfide.

Nitrogen Chelation onto Uranyl & Selectivity

Hancock and colleagues[21] looked at the variability of sulfur and nitrogen-based ligands. The group used commonly found ligands (Figure 5) to see which ones had selectivity towards various lanthanides and actinides, including different oxidation states and coordinating sites of the same element. They primarily looked at acidity, basicity, ΔH, and ΔG values (Gibbs free energy of the reaction). This research provided a lot of insight into which ligands would chelate best to specific ions.

This group heavily focused on nitrogen-based ligands. 14 out of the 15 ligands they used were nitrogen-based, with the last one being a sulfur-based ligand. They found that, especially with the sulfur-based chelation, it produced a good correlation with the free energy values for forming a thioether complex. Adversely, it was found that thioethers have very weak coordination to Ac and Ln(III) cations. Their findings for monoamine's and pyridyl type donors were that they have an affinity for M(II) ions; this includes UO_2.

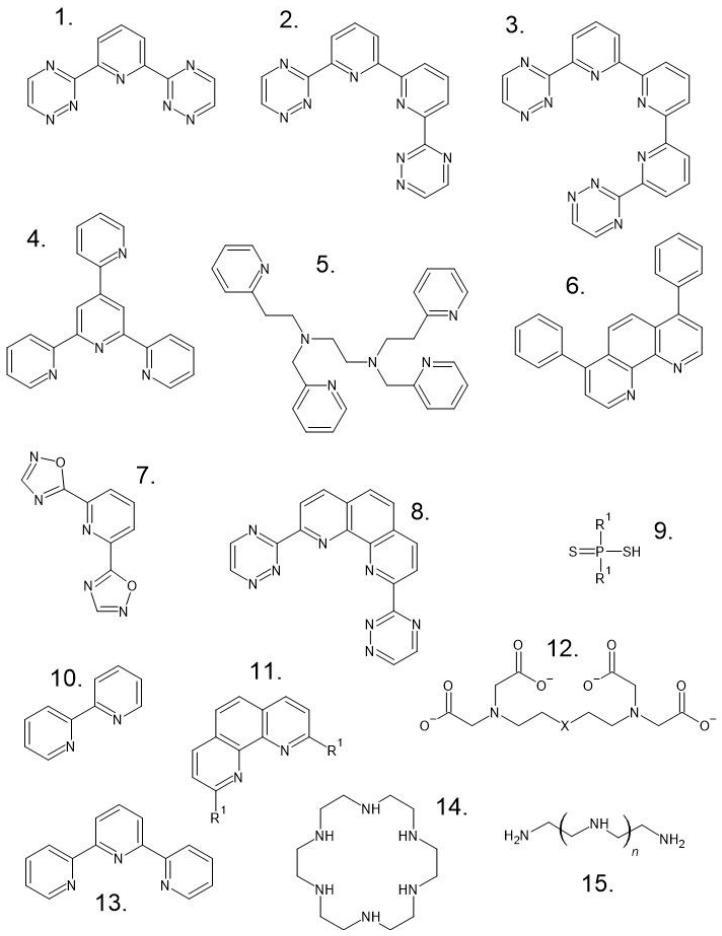

Figure 5. Hancock Ligands: 1. BTP, 2. BTB, 3. BTTP, 4. TPTZ, 5. TPEN, 6. Di-phenyl-phen, 7. ODP, 8. BTphen, 9. L1, 10. BIPY, 11. phen/PDAM/PDA/PDALC/DPP, 12. TEDTA/EEDTA, 13. TPY, 14. 18-ane-N_6, 15. dien/trien/tetren/...

Substituent Effects

Guillaumont et al.[22] in 2006 published a paper that revolved around how different substituents affected bond distance. They were primarily working with Terpyridine (TERPY), bis(1,2-4-triazin-3-yl)pyridine (R-BTP), and 2-amino-4,6-di-(pyridin-2-yl)-1,3,5-triazine (ADPTZ) ligands as seen in Figure 6. Unlike the previous papers, there isn't a uranyl ion mentioned here. Instead, they work with a U(III) that is attached to one of the three ligands in Figure. Moreover, it then varies further with the rest of the coordination sites being occupied by either Cl, H_2O, and Cl, or H_2O

and NO_3.

Their findings were pretty clear for U(VI). As they added electron-withdrawing groups, like cyanide, the bond distance between the grew longer. Electron donor groups had the reverse effect. They shortened the metal-ligand bond distance.

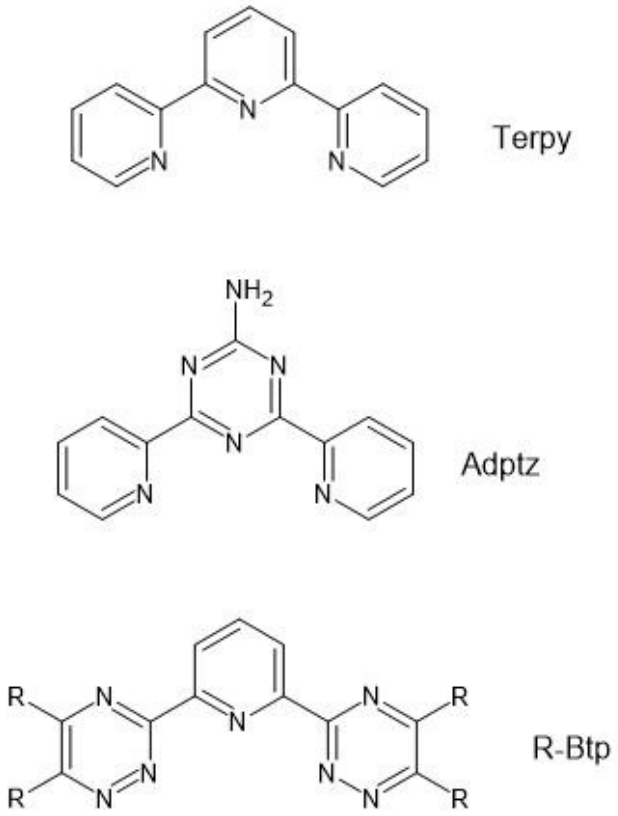

Figure 6. Guillaumont Ligands.

Goals

We would like to study the coordination chemistry and reaction energetics of uranyl complexes with ethylenediamine, 1,2-ethanedithiol, and cysteamine ligands using density functional level (DFT) of theory. These three base ligands were selected because of the soft atom chelation selectivity and the lack of literature around sulfur-based ligands. Nitrogen and sulfur are both very promising for targeting UO_2^{2+}. It is our hope to see if this targeting can be improved while simultaneously gathering more information on various sulfur ligands. Additionally, the C-C backbone in each of the base ligands provides a platform to observe the effects of various substituents in different positioning. The electron withdrawal or donation ability of the substituents will have an interesting effect. There isn't substantial information in the literature indicating what that effect may be or if the substituents will have the same effect in both nitrogen and sulfur chelation. Our hopes are to find out if they play a similar role in both, and if not, see exactly why.

Coordination preferences and structural changes of the uranyl complexes based on the chelating atom (nitrogen versus sulfur), substituent group (CH_3, CN, OCH_3, and Cl), and the position of the substituent on the ligand will be studied. Thermodynamic parameters, including Gibbs free energy of the reaction and enthalpy change, will be evaluated for each chelation reaction. Additionally, bond angle (L-M-L) and bond distance (M-L) will be measured to see if there are any substantial differences in the various ligands. These parameters were chosen to provide the most insight into the uranium extraction process.

We are expecting the electron-withdrawing and donating ability of our chosen substituents to play a major role in the overall $\Delta G_{reaction}$. Based on previous research, It's expected that the electron-donating groups such as methyl will lower the $\Delta G_{reaction}$ and electron-withdrawing groups will have an adverse effect. Additionally, the positioning of these substituents is predicted to have a higher effect in the equatorial position rather than the axial because it is lying within the same plane.

CHAPTER TWO: EXPERIMENTAL

2.1 Computational Parameters

Computational studies were performed at the density functional level of theory using G09W (Gaussian) computational package with Gauss View 5.0 graphical interface[23]. Geometry optimization and frequency calculations were carried out using B3LYP hybrid functional to find the minimum energy structure without any geometry constraints. The optimization portion gives the proper structure and a stationary point, and the frequency calculation can be used to calculate the vibrational modes and energies. Thermodynamic properties[24], including Gibbs free energy and enthalpy, can be calculated after both frequency and optimization have converged. A split basis set was chosen to accommodate the uranium (f block) and the soft atoms (s and p block). The Stuttgart basis set was chosen for the uranium metal ion with a Stuttgart effective core potential (ECP): 60 of its electrons are in the core. 6-311G(d,p) basis set was given to the soft atoms (H, C, N, O, S, Cl).

2.2 Project Design

2.2.1 Uranium complex calculations

1) Base structure $UO_2(H_2O)_5$, was built using GausView graphical interface. 2) Two water molecules adjacent to each other were removed, and one of the bidentate foundation molecules (ethylenediamine, 1,2-ethanedithiol, or cysteamine) replaced them. 3) One of the 59 possible structures from Table 1 was chosen and built. 4) The calculation was run under a freq+opt command with the method being ground state DFT default spin B3LYP. A split basis set was needed; Stuttgart for the uranium and 6-311G(d,p) for the soft atoms. Also, an effective core potential was used for the uranium.

2.2.2 Ligand calculations

1) A ligand from Table 1 was chosen and built using GausView graphical interface 2) It was ran under a freq+opt with the method being ground state DFT default spin B3LYP. The basis used

was 6-311G (d,p).

Figure 7 depicts the iterative process for ensuring that all of the calculations converged and that data was collected efficiently. After picking a ligand, building it, applying the compositional parameters, and assigning a checkpoint location, there's a possibility of three total outcomes; 1) the job fully completed with the optimization and the frequency both converging. If this was the case, then the information was gathered, and the cycle continued 2) if the geometry converged, but the frequency didn't, then we applied force constants to the partially converged checkpoint (.chk) file and resubmitted the job 3) similarly, if both the geometry and the frequency didn't converge, then we checked our model and our parameters, and we reran the job.

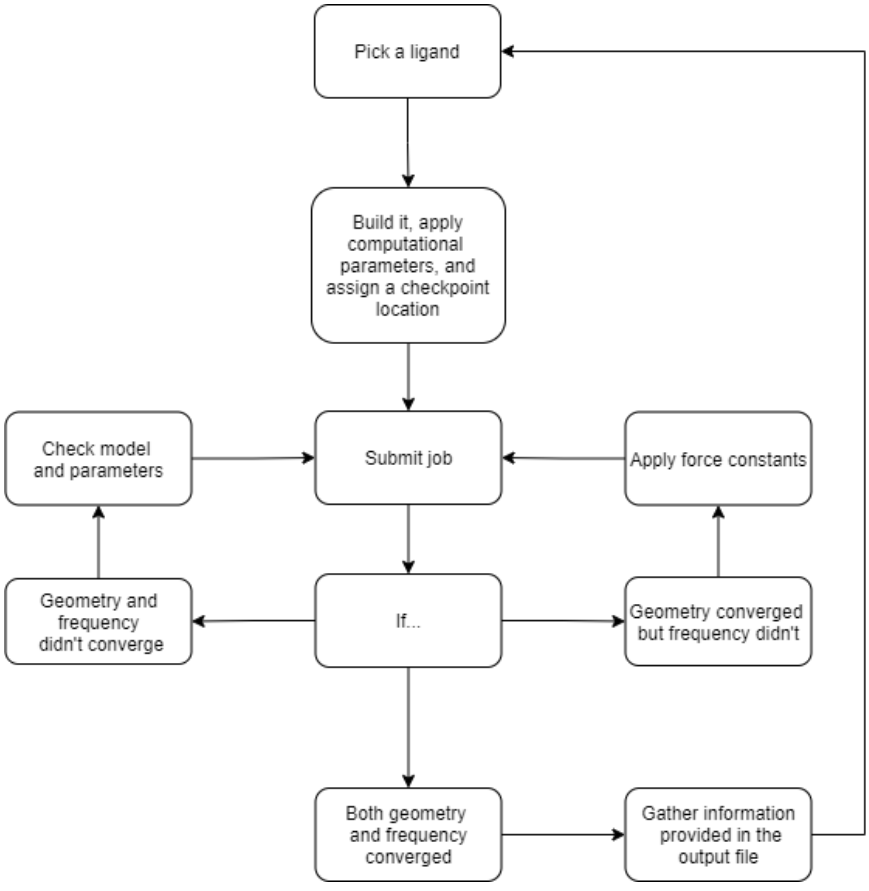

Figure 7. Iterative diagram for calculations

Table 1. Ligand variations. Prime(') denotes which atom the numbering begins with; no prime indicates the sulfur atom is the first, then if there is a prime, this indicates the nitrogen is the first atom. Prime is only used for cysteamine because it has two different chelating atoms.

Substituent (R)	Base Ligand	# of R	Position	Name
N/A	EDA	N/A	N/A	EDA
N/A	EDA-S-1	N/A	N/A	EDA-S-1
N/A	EDA-S-2	N/A	N/A	EDA-S-2
CH3	EDA	1	Eq	EDA-CH3-1-Eq
OCH3	EDA	1	Eq	EDA-OCH3-1-Eq
CN	EDA	1	Eq	EDA-CN-1-Eq
Cl	EDA	1	Eq	EDA-Cl-1-Eq
CH3	EDA	1	Ax	EDA-CH3-1-Ax
OCH3	EDA	1	Ax	EDA-OCH3-1-Ax
CN	EDA	1	Ax	EDA-CN-1-Ax
Cl	EDA	1	Ax	EDA-Cl-1-Ax
CH3	EDA	2	Ax-Eq	EDA-CH3-2-Ax-Eq
OCH3	EDA	2	Ax-Eq	EDA-OCH3-2-Ax-Eq
CN	EDA	2	Ax-Eq	EDA-CN-2-Ax-Eq
Cl	EDA	2	Ax-Eq	EDA-Cl-2-Ax-Eq
CH3	EDA	2	Eq-Eq	EDA-CH3-2-Eq-Eq
OCH3	EDA	2	Eq-Eq	EDA-OCH3-2-Eq-Eq
CN	EDA	2	Eq-Eq	EDA-CN-2-Eq-Eq
Cl	EDA	2	Eq-Eq	EDA-Cl-2-Eq-Eq
CH3	EDA-S-1	1	Eq	EDA-S-1-CH3-1-Eq
OCH3	EDA-S-1	1	Eq	EDA-S-1-OCH3-1-Eq
CN	EDA-S-1	1	Eq	EDA-S-1-CN-1-Eq
Cl	EDA-S-1	1	Eq	EDA-S-1-Cl-1-Eq
CH3	EDA-S-1	1	Ax	EDA-S-1-CH3-1-Ax
OCH3	EDA-S-1	1	Ax	EDA-S-1-OCH3-1-Ax
CN	EDA-S-1	1	Ax	EDA-S-1-CN-1-Ax
Cl	EDA-S-1	1	Ax	EDA-S-1-Cl-1-Ax
CH3	EDA-S-1'	1	Eq	EDA-S-1'-CH3-1-Eq
OCH3	EDA-S-1'	1	Eq	EDA-S-1'-OCH3-1-Eq
CN	EDA-S-1'	1	Eq	EDA-S-1'-CN-1-Eq
Cl	EDA-S-1'	1	Eq	EDA-S-1'-Cl-1-Eq
CH3	EDA-S-1'	1	Ax	EDA-S-1'-CH3-1-Ax
OCH3	EDA-S-1'	1	Ax	EDA-S-1'-OCH3-1-Ax
CN	EDA-S-1'	1	Ax	EDA-S-1'-CN-1-Ax
Cl	EDA-S-1'	1	Ax	EDA-S-1'-Cl-1-Ax
CH3	EDA-S-1	2	Ax-Eq	EDA-S-1-CH3-2-Ax-Eq
OCH3	EDA-S-1	2	Ax-Eq	EDA-S-1-OCH3-2-Ax-Eq
CN	EDA-S-1	2	Ax-Eq	EDA-S-1-CN-2-Ax-Eq
Cl	EDA-S-1	2	Ax-Eq	EDA-S-1-Cl-2-Ax-Eq
CH3	EDA-S-1	2	Eq-Eq	EDA-S-1-CH3-2-Eq-Eq
OCH3	EDA-S-1	2	Eq-Eq	EDA-S-1-OCH3-2-Eq-Eq
CN	EDA-S-1	2	Eq-Eq	EDA-S-1-CN-2-Eq-Eq
Cl	EDA-S-1	2	Eq-Eq	EDA-S-1-Cl-2-Eq-Eq
CH3	EDA-S-2	1	Eq	EDA-S-2-CH3-1-Eq
OCH3	EDA-S-2	1	Eq	EDA-S-2-OCH3-1-Eq
CN	EDA-S-2	1	Eq	EDA-S-2-CN-1-Eq
Cl	EDA-S-2	1	Eq	EDA-S-2-Cl-1-Eq
CH3	EDA-S-2	1	Ax	EDA-S-2-CH3-1-Ax
OCH3	EDA-S-2	1	Ax	EDA-S-2-OCH3-1-Ax
CN	EDA-S-2	1	Ax	EDA-S-2-CN-1-Ax
Cl	EDA-S-2	1	Ax	EDA-S-2-Cl-1-Ax
CH3	EDA-S-2	2	Ax-Eq	EDA-S-2-CH3-2-Ax-Eq
OCH3	EDA-S-2	2	Ax-Eq	EDA-S-2-OCH3-2-Ax-Eq
CN	EDA-S-2	2	Ax-Eq	EDA-S-2-CN-2-Ax-Eq
Cl	EDA-S-2	2	Ax-Eq	EDA-S-2-Cl-2-Ax-Eq
CH3	EDA-S-2	2	Eq-Eq	EDA-S-2-CH3-2-Eq-Eq
OCH3	EDA-S-2	2	Eq-Eq	EDA-S-2-OCH3-2-Eq-Eq
CN	EDA-S-2	2	Eq-Eq	EDA-S-2-CN-2-Eq-Eq
Cl	EDA-S-2	2	Eq-Eq	EDA-S-2-Cl-2-Eq-Eq

2.3 Substituent Positioning

Only the hydrogens on the carbons were replaced by the substituents: methyl (CH_3), Methoxy (OCH_3), Cyanide (CN), and Halogen (Cl). There are four possible positions, with two of them being equatorial and two being axial. Moreover, it was hypothesized that the equatorial hydrogens would have more of a substantial impact due to transannular strain. This is because the way our ligand is bound to the metal center, creates a five-member "ring" with one of the two carbons acting like the envelope flap. The substituent, when in the axial position, intrudes over into the space of the complex and creates strain. This is the primary reason why we chose equatorial-equatorial and not axial-axial; we felt we could observe the maximum effect this way. Referencing Figure 8, the molecules with only one substituent always substitute on the carbon labeled "2."

Calculations

Gibb's free energy and enthalpy were both calculated computationally for the individual complexes and ligands, but entropy was not. Entropy was calculated using the Gibbs free energy equation (Equation 8). Gibb's free energy was originally given in Hartree/particle and had to be converted to kJ/mol. This was done by multiplying the value by 2625.5 kj*particle/Hartree*mol and changing the units to kJ/mol.

$$\Delta G = \Delta H - T\Delta S \tag{8}$$

where ΔG is Gibbs free energy, ΔH is enthalpy, ΔS is entropy, and T is temperature. The free energy of the reaction still needed to be calculated. Equations 10 & 11 were used to calculate the $\Delta G_{reaction}$.

$$UO_2(H_2O)_5 + L \rightarrow UO_2(H_2O)_3L + 2H_2O \tag{9}$$

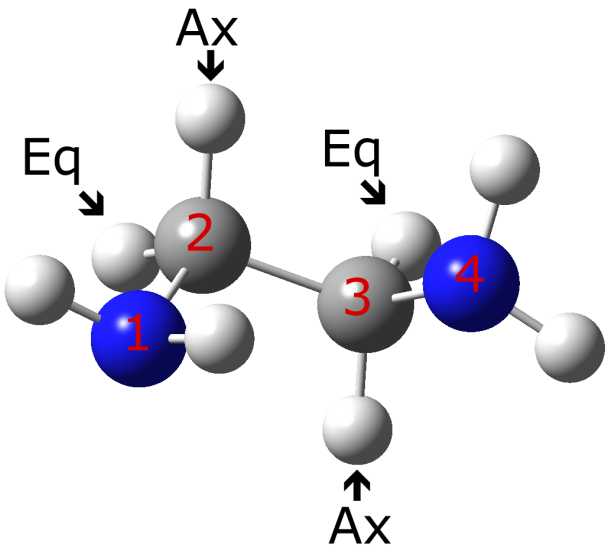

Figure 8. Numbered ethylenediamine (EDA) with explicit labels on the hydrogen atoms attached to the carbon.

Figure 9. Reaction of penta aqua saturated uranyl complex undergoing a bidentate ligand substitution

To find $\Delta G_{reaction}$ we used:

$$\Delta G_{reaction} = \sum G_{products} - \sum G_{reactants} \tag{10}$$

An example incorporating numerical values using ethylenediamine can be found below:

$$\begin{aligned}
\Delta G_{reaction} &= \sum G_{products} - \sum G_{reactants} \\
&= (G_{UO_2(H_2O)_3EDA} + 2G_{H_2O}) - (G_{UO_2(H_2O)_5} + G_{EDA}) \\
&= (-1047.011229 + 2(-76.443769)) - (-1009.373475 + (-190.49553)) \\
&= -0.029762 Hartree/particle \\
&= -78.140131 kJ/mol
\end{aligned} \tag{11}$$

Gibbs's free energy values for the four different molecules were taken, and the products were added together and subtracted from the sum of the reactants. This gives the overall change in Gibbs free energy for our reaction.

Enthalpy was calculated in a similar manner. Four enthalpy values were taken from the calculations, two of them were the products, and two of them were the reactants. The products are added together, and the reactants were added together, then the sums were subtracted. After multiplying by 2625.5 kj*particle/Hartree*mol, this gave us ΔH. Finally, the calculations were run at 298.15K and 1 atm pressure. Plugging all of this information into Equation 8 gives us entropy.

CHAPTER THREE: RESULTS AND DISCUSSION

Below you will find subsections on the various correlations between ethylenediamine, cysteamine, and 1,2-ethanedithiol complexes and their differences. Data from the structural parameters of the complexes and their associated ligands can be found in Tables 2-4. Tables 5-7 show the energy, enthalpy, and entropy values for our complexes. Energy and entropy were calculated using Equation 10, and entropy was calculated using Equation 8. Some of the subsections have calculations where the R-C (R=S,N) bond is disassociated during optimization. We are unsure of the reasoning why this happened: the bond distance between the two atoms didn't change significantly (at most, it changed by a hundredth of an Angstrom) from the initial structure. Because of this, we found it to be negligible and continued with the experiment.

3.1 Geometrical Properties

Various bond distances were recorded and analyzed. Most notably among them were the ligand-metal bond distances and ligand-metal-ligand bond angles. Additionally, the three water molecules bond distances (L-M) were also recorded and used in Figure 10 as a reference. It was important to track the distances of the water ligands to ensure that they stated within the distance to be considered a bond. If they were to exceed the maximum bond distance from the uranium metal center, then it would no longer be $UO_2(H_2O)_3$.

Figures 11-14 show the bond distances (in Angstroms) of atoms 1 and 2. These are the metal-ligand bonds, either U-N or U-S. As electron donor groups, such as methyl, were added to the foundation molecule, the bond distance decreased and when electron-withdrawing substituents were added, such as chlorine, the bond distance increased. This matches exactly what the literature found[22]. We believe this is because it made the electron pair on either the sulfur or the nitrogen more readily available. Because the bond between the metal and the chelating atoms is considered a dative bond, the electron lone pair plays a crucial role in determining the bond distance.

Figure 15 has the bond distances of water molecules A, B, and C. There is a slight downward shift in the bond distance when going from ethylenediamine complexes to 1,2-ethanedithiol. This means that the metal center became electron-deficient and needed additional support from the water molecules.

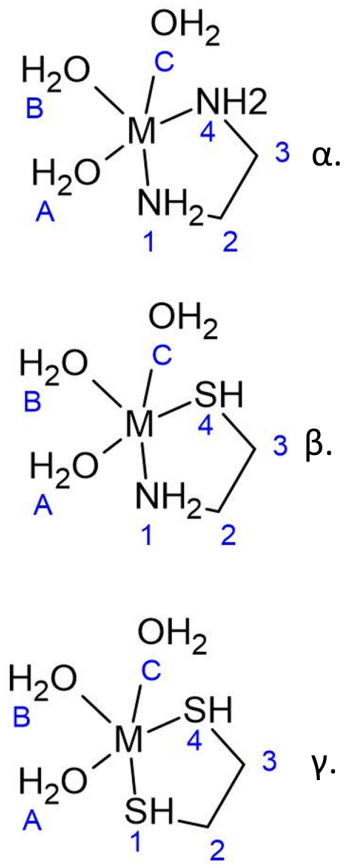

Figure 10. Bond distance reference. Ethylenediamine (top), Cysteamine (middle), and 1,2-Ethanedithiol (top)

Table 2. Bond distances (Å) and angle (°) for ethylenediamine (α.) complexes

α.		Å	Å	Å	Å	Å
Name	Bond Angle (L-M-L)	Atom 1	Atom 4	A	B	C
EDA	66.23424	2.5821	2.5821	2.5163	2.5163	2.5162
EDA-CH3-1-Eq	65.94524	2.56841	2.57768	2.51613	2.52063	2.51662
EDA-OCH3-1-Eq	65.93666	2.56734	2.57454	2.51787	2.51966	2.51903
EDA-CN-1-Eq	65.45158	2.60195	2.59478	2.51302	2.5068	2.5078
EDA-Cl-1-Eq	65.48357	2.59961	2.59112	2.51354	2.50936	2.50877
EDA-CH3-1-Ax	65.99705	2.57787	2.5743	2.51737	2.51785	2.51773
EDA-OCH3-1-Ax	65.75782	2.58972	2.57071	2.51763	2.51609	2.51518
EDA-CN-1-Ax	65.41482	2.62233	2.5989	2.51203	2.50432	2.50746
EDA-Cl-1-Ax	65.46587	2.61361	2.59087	2.51367	2.50631	2.50844
EDA-CH3-2-Ax-Eq	65.78176	2.57375	2.56261	2.51912	2.52024	2.51726
EDA-OCH3-2-Ax-Eq	65.79389	2.59309	2.56549	2.51977	2.51773	2.51039
EDA-CN-2-Ax-Eq	64.82236	2.639	2.61905	2.50724	2.49479	2.50128
EDA-Cl-2-Ax-Eq	64.97394	2.62667	2.60817	2.50935	2.49912	2.50403
EDA-CH3-2-Eq-Eq	65.32987	2.55813	2.55807	2.52083	2.52317	2.52081
EDA-OCH3-2-Eq-Eq	65.62863	2.55742	2.56462	2.51781	2.52196	2.51989
EDA-CN-2-Eq-Eq	64.60405	2.61063	2.61064	2.50616	2.49825	2.50616
EDA-Cl-2-Eq-Eq	64.29066	2.59923	2.59923	2.50875	2.50297	2.50875

Table 3. Bond distances and angles for cysteamine (β.) complexes

β.		Å	Å	Å	Å	Å
Name	Bond Angle (L-M-L)	Atom 1	Atom 4	A	B	C
EDA-S-1	66.80621	2.59061	2.98175	2.5013	2.5007	2.5160
EDA-S-1-CH3-1-Eq	66.64028	2.59004	2.96151	2.51868	2.50433	2.5007
EDA-S-1-OCH3-1-Eq	66.78189	2.59243	2.92221	2.53106	2.50939	2.49706
EDA-S-1-CN-1-Eq	66.41733	2.60648	2.995	2.51058	2.49374	2.49617
EDA-S-1-Cl-1-Eq	66.53751	2.60345	2.98356	2.51185	2.49751	2.49805
EDA-S-1-CH3-1-Ax	66.83483	2.58119	2.96584	2.52007	2.5046	2.50285
EDA-S-1-OCH3-1-Ax	67.47059	2.5841	2.95576	2.52306	2.50816	2.5024
EDA-S-1-CN-1-Ax	66.8714	2.61576	3.01735	2.50475	2.4921	2.49751
EDA-S-1-Cl-1-Ax	66.5377	2.60072	2.99753	2.50981	2.49606	2.50033
EDA-S-1'-CH3-1-Eq	66.57978	2.57734	2.97373	2.51793	2.50397	2.50375
EDA-S-1'-OCH3-1-Eq	66.48433	2.57273	2.98581	2.51238	2.5018	2.50349
EDA-S-1'-CN-1-Eq	66.10124	2.6071	2.99581	2.51222	2.49169	2.4954
EDA-S-1'-Cl-1-Eq	66.21422	2.60574	2.99072	2.51324	2.49389	2.49646
EDA-S-1'-CH3-1-Ax	66.56473	2.59655	2.97372	2.51433	2.50289	2.50011
EDA-S-1'-OCH3-1-Ax	64.71091	2.75614	3.04648	2.51109	2.49182	2.48984
EDA-S-1'-CN-1-Ax	65.75448	2.63985	3.0058	2.51148	2.48782	2.49213
EDA-S-1'-Cl-1-Ax	65.9021	2.64075	2.99593	2.51244	2.48955	2.49126
EDA-S-1-CH3-2-Ax-Eq	66.55389	2.57416	2.96026	2.5186	2.50726	2.5025
EDA-S-1-OCH3-2-Ax-Eq	67.72212	2.57347	2.97232	2.51601	2.50941	2.50327
EDA-S-1-CN-2-Ax-Eq	66.34616	2.63904	3.03055	2.50045	2.48408	2.4937
EDA-S-1-Cl-2-Ax-Eq	66.40412	2.62418	3.00602	2.50476	2.49058	2.49575
EDA-S-1-CH3-2-Eq-Eq	65.80812	2.57323	2.94878	2.5228	2.5073	2.50089
EDA-S-1-OCH3-2-Eq-Eq	66.66419	2.57441	2.92765	2.5259	2.51111	2.50197
EDA-S-1-CN-2-Eq-Eq	65.26928	2.61652	3.00553	2.50933	2.48563	2.49027
EDA-S-1-Cl-2-Eq-Eq	65.0934	2.60576	2.98348	2.51341	2.49157	2.49251

Table 4. Bond distances and angles for 1,2-ethanedithiol (γ.) complexes

γ.		Å	Å	Å	Å	Å
Name	Bond Angle (L-M-L)	Atom 1	Atom 4	A	B	C
EDA-S-2	67.94037	3.0037	3.00367	2.4941	2.4849	2.4942
EDA-S-2-CH3-1-Eq	67.67849	2.98085	3.00037	2.49623	2.48654	2.49779
EDA-S-2-OCH3-1-Eq	66.72814	2.93551	3.00173	2.4868	2.49383	2.51141
EDA-S-2-CN-1-Eq	67.39661	3.00738	3.02239	2.49305	2.47703	2.4911
EDA-S-2-Cl-1-Eq	67.19137	2.99299	3.0224	2.49437	2.48055	2.49202
EDA-S-2-CH3-1-Ax	67.97746	2.98972	2.99811	2.49442	2.4872	2.49623
EDA-S-2-OCH3-1-Ax	68.62492	2.9705	3.01735	2.49358	2.49085	2.50026
EDA-S-2-CN-1-Ax	66.8009	3.04183	3.04365	2.49039	2.47549	2.48379
EDA-S-2-Cl-1-Ax	66.90965	3.02132	3.02941	2.49198	2.47922	2.4876
EDA-S-2-CH3-2-Ax-Eq	67.61203	2.98503	2.97687	2.49852	2.48933	2.49905
EDA-S-2-OCH3-2-Ax-Eq	68.6053	2.98926	2.96974	2.50369	2.49695	2.49611
EDA-S-2-CN-2-Ax-Eq	66.76222	3.05122	3.05795	2.48927	2.46847	2.48464
EDA-S-2-Cl-2-Ax-Eq	67.23298	3.02946	3.02316	2.49268	2.47598	2.49124
EDA-S-2-CH3-2-Eq-Eq	66.80914	2.97433	2.97433	2.49754	2.49077	2.49749
EDA-S-2-OCH3-2-Eq-Eq	65.27915	2.96029	2.94314	2.49271	2.50094	2.50347
EDA-S-2-CN-2-Eq-Eq	66.69377	3.02372	3.02372	2.48951	2.4715	2.48951
EDA-S-2-Cl-2-Eq-Eq	66.19893	3.00243	3.00243	2.49237	2.47801	2.492371

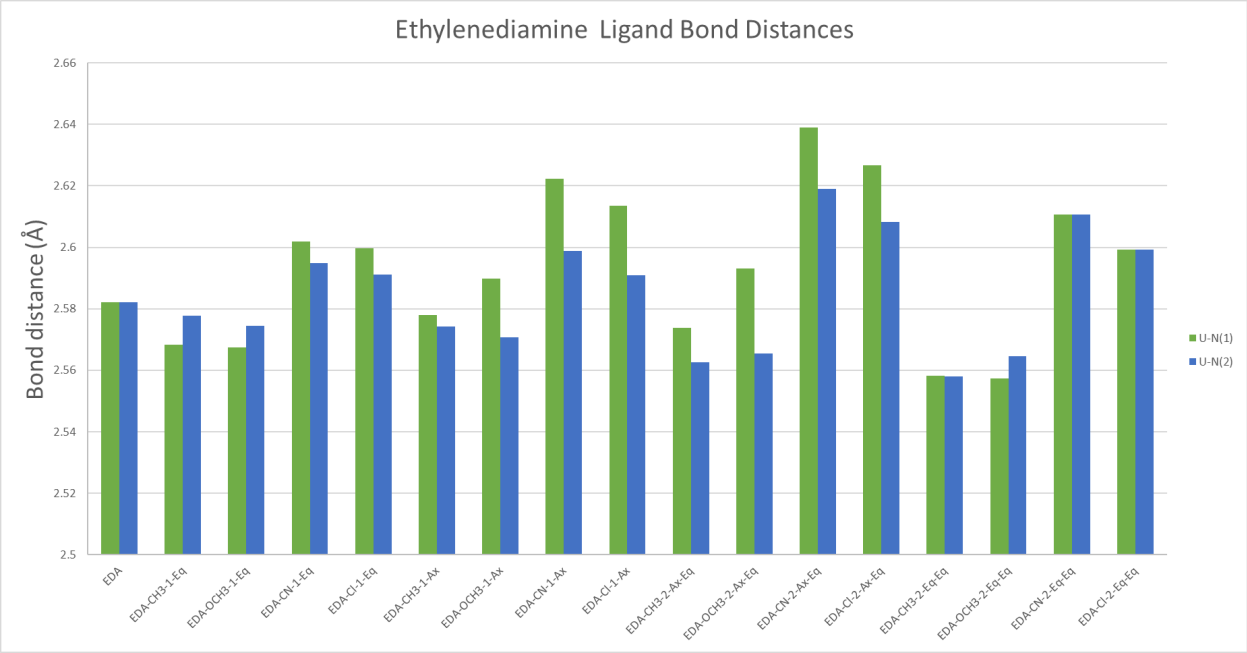

Figure 11. Bond distances (Å) of ethylenediamine ligands (M-L)

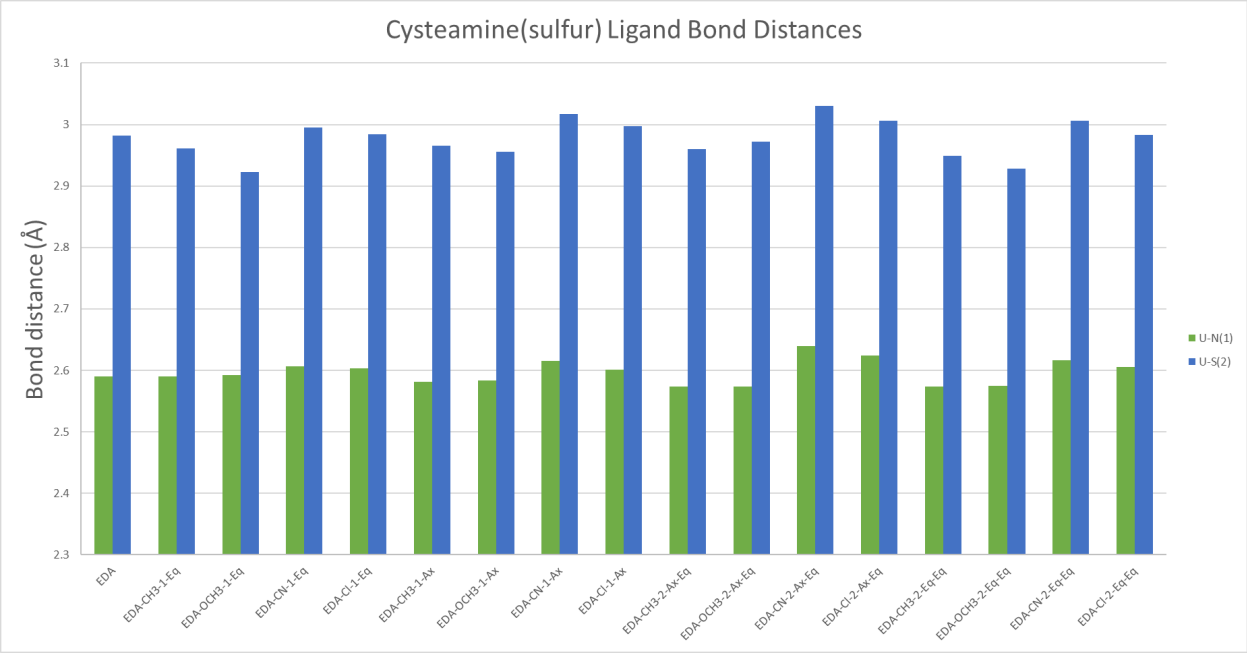

Figure 12. Bond distances (Å) of cysteamine (sulfur) ligands (M-L)

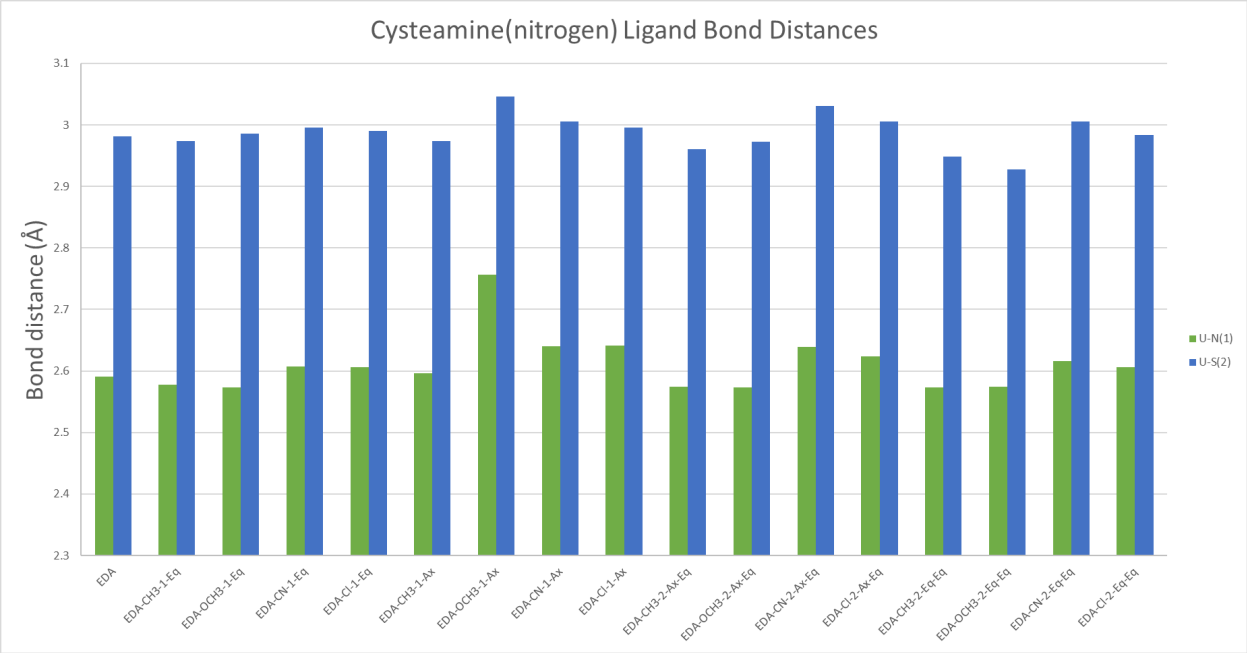

Figure 13. Bond distances (Å) of cysteamine (nitrogen) ligands (M-L)

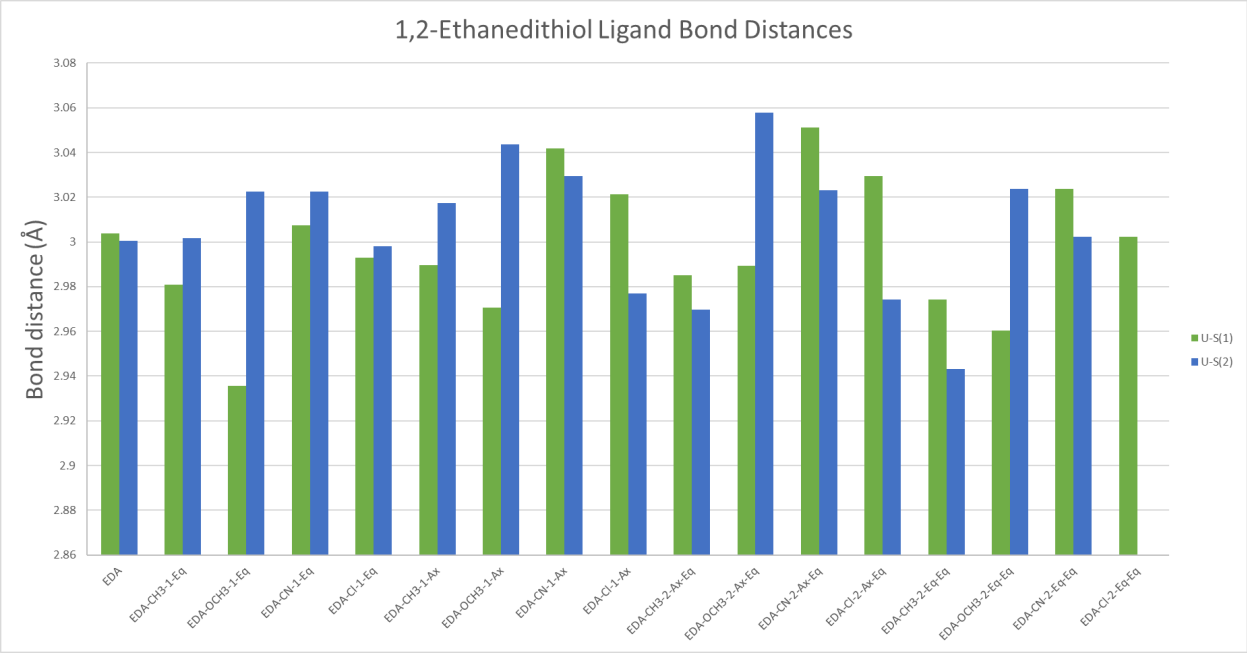

Figure 14. Bond distances (Å) of 1,2-ethanedithiol ligands (M-L)

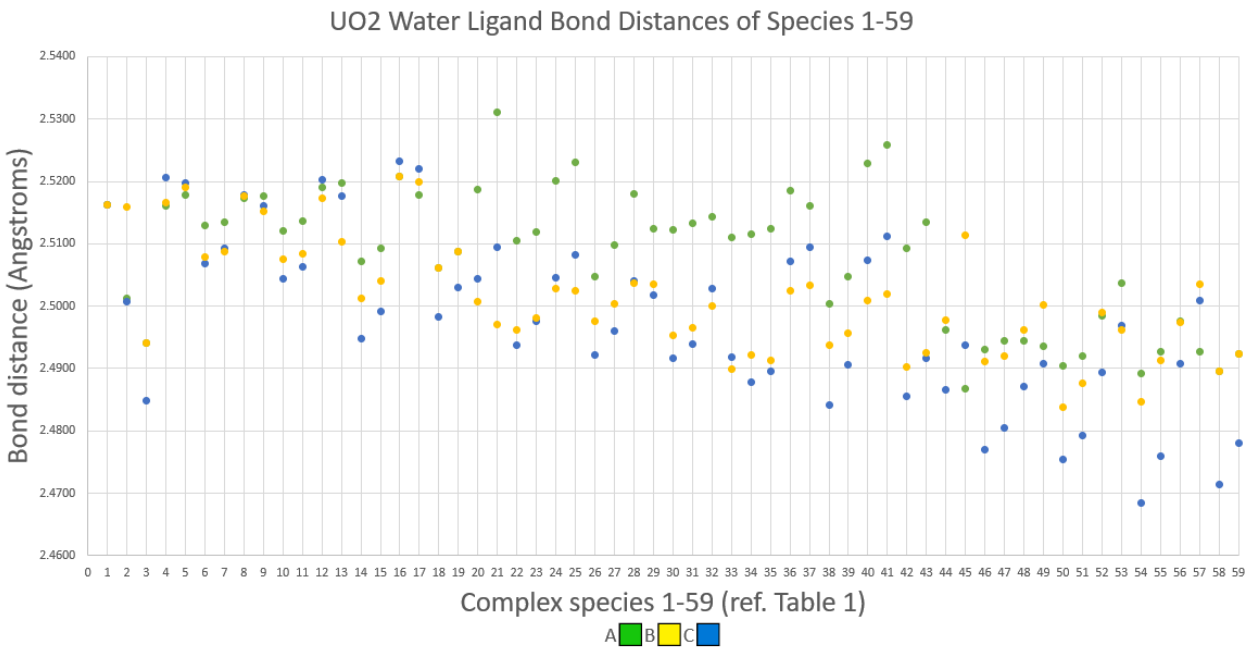

Figure 15. U-O bond distances of water molecules A, B, and C

3.2 Positioning

Figures 16-19 show a comparison between axial and equatorial positioning of ethylenediamine, cysteamine (nitrogen variant), cysteamine (sulfur variant), and 1,2-ethanedithiol complexes. In these comparisons, the substituent is shown in either the equatorial or the axial position. There wasn't a common trend found in positioning, and depending on the substituent, it had a different effect. Looking closer at an example, Figure 16 depicts ethylenediamine with one substituent(ethylenediamine is our foundation molecule shown in green). The four different substituents are side-by-side: CH_3 in the dark blue and orange, OCH_3 in burnt orange and gray, CN in dark gray and yellow, Cl in brown and blue. We notice that depending on the substituent; the positioning can either increase or decrease the energy value ($\Delta G_{reaction}$).

At first, this perturbed us because it didn't fit with the original hypothesis. But upon further observation, the ligands that we used have a similar shape to a cyclopentane envelope where there

is a ”lip.” One of the commonalities in cyclic structures is a ring strain. This is due to the bond angles having to find an equilibrium at the lowest possible energy. The energy differences here can most likely be attributed to transannular strain. The methyl group in the equatorial position (Figure 32) is favored because of the lack of hydrogen crowding shown in the axial position (Figure 36).

Similar observations were made for Figures 17-19. There wasn't a common trend between the positioning. Especially when considering the methoxy substituent, depending on the foundation molecule it either substantially increased or decreased the $\Delta G_{reaction}$. This means that for future research regarding multi-hydrogen ligands, both positions will need to be tested independently to see which results in the lowest $\Delta G_{reaction}$ value.

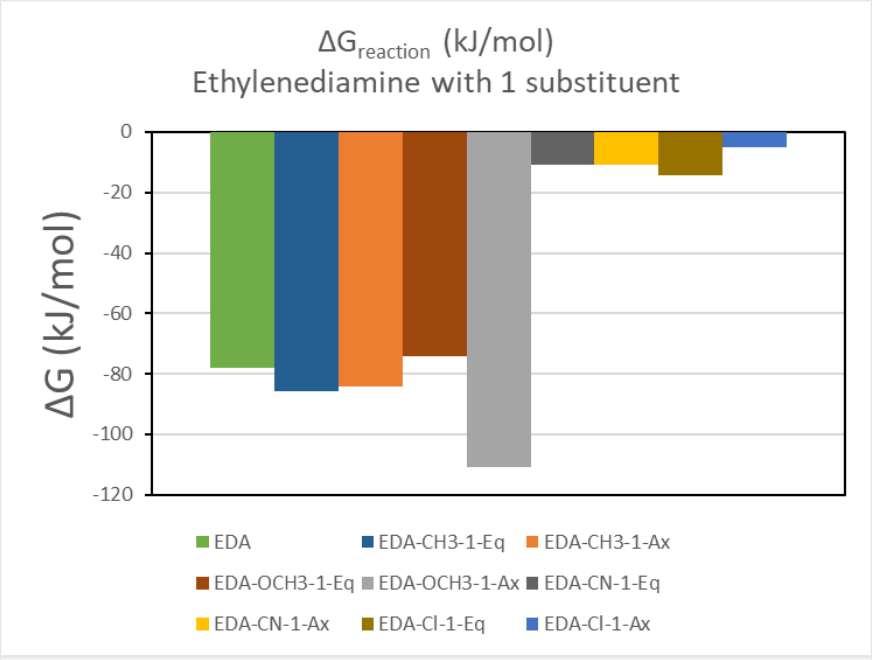

Figure 16. $\Delta G_{reaction}$ values of ethylenediamine with one substituent

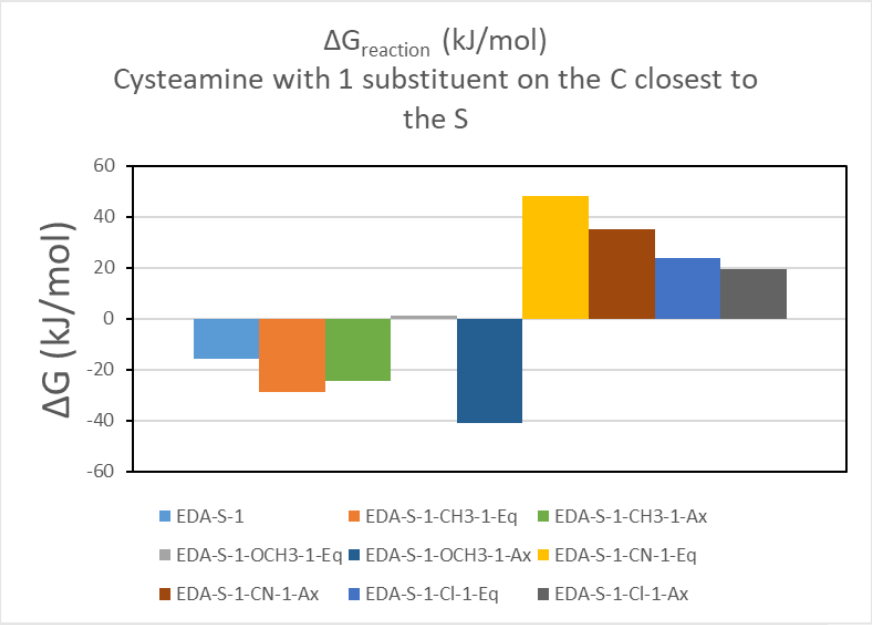

Figure 17. $\Delta G_{reaction}$ values of cysteamine (sulfur) with one substituent

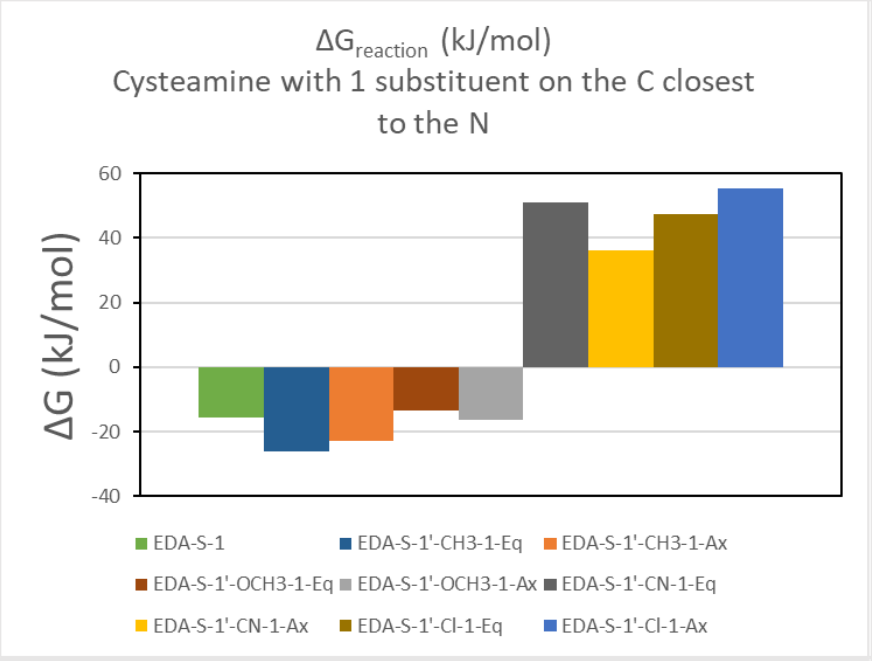

Figure 18. $\Delta G_{reaction}$ values of cysteamine (nitrogen) with one substituent

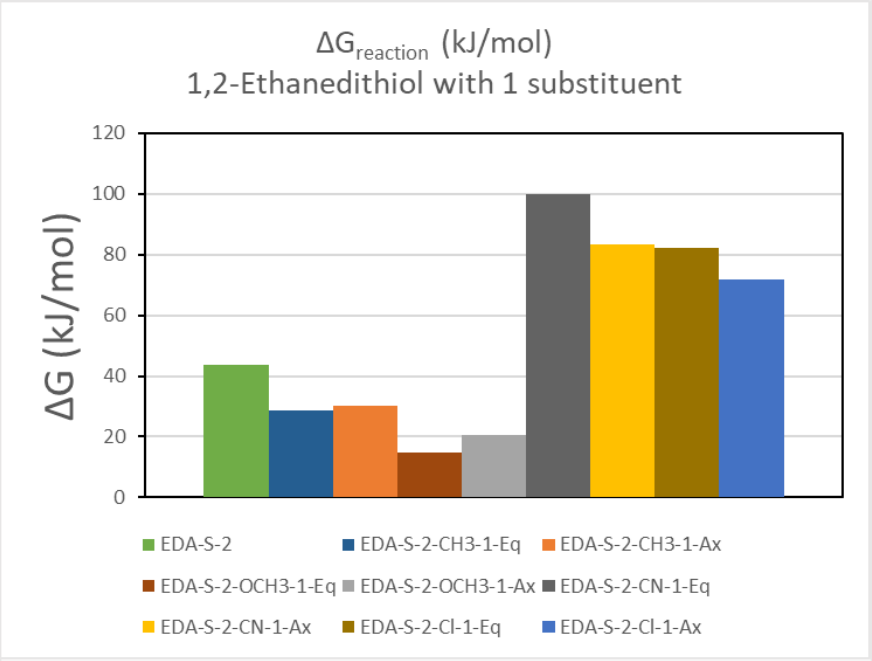

Figure 19. $\Delta G_{reaction}$ values to 1,2-ethanedithiol with one substituent

3.3 Ligand Chelation Comparison

We noticed a significant change in the reaction free energy regarding ethylenediamine (Figure 29), cysteamine (Figure 30), 1,2-ethanedithiol (Figure 31). This is visually realized in Figure 20. Initially, ethylenediamine had a $\Delta G_{reaction}$ of -78.14kJ/mol. When sulfur was substituted for one of the nitrogens, it grew tremendously in the positive direction to -15.61kJ/mol. Finally, when the second nitrogen was substituted for sulfur, it rose further to 43.72kJ/mol. Just this data set indicates that nitrogen-based ligands are far more spontaneous and likely to be a good candidate for further research for uranyl coordination chemistry.

In the Townsend paper[20], there was a formation of a sulfur-based ligand (persulfide S_2). While their condition was slightly varied from ours, it looked to be a promising indicator for research and development. We believe that the reason why our sulfur-based ligands had high reaction Gibbs free energy values was due to steric hindrance from the hydrogen atoms attached directly

to the sulfur. This can cause strain on the complex, thus increasing the energy.

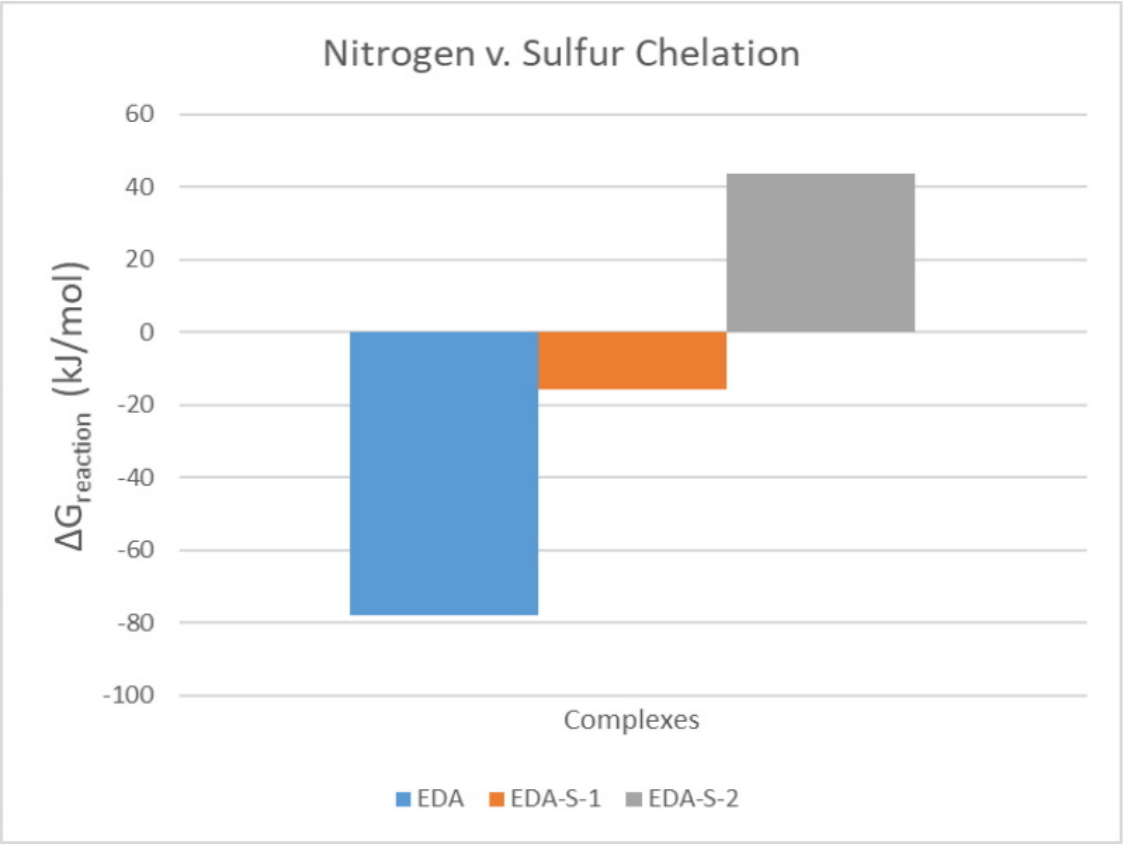

Figure 20. $\Delta G_{reaction}$ variation: nitrogen v. sulfur chelation

3.4 Substituent Effects

Figures 21-24 display $\Delta G_{reaction}$ values for ethylenediamine, cysteamine (both variants), and 1,2-ethanedithiol complexes with a single substituent in the equatorial position. There is a common trend among the substituents and their $\Delta G_{reaction}$ values. After substituting with a strong electron donor group, like a methyl group, the overall $\Delta G_{reaction}$ is lowered from the base value of the foundation molecule. Moreover, When substituting with an electron-withdrawing group such as cyanide or halogen, in this case, chlorine, the $\Delta G_{reaction}$ drastically increases from the base value.

The only varying factor in this comparison is the substituents. The positioning and the number of substituents remain consistent. Looking closer at an example, Figure 21 has the foundation molecule ethylenediamine colored light blue and is shifted to the left. Its energy value is slightly less than -80 kJ/mole. We can see that when a methyl (CH_3) group, shown in orange, replaces one of the hydrogens that the energy value decreases below ethylenediamine's value. Methoxy (OCH_3), established in gray, didn't have a noticeable impact and hovered around the same value as ethylenediamine. However, cyanide (CN) and chlorine (Cl), shown in yellow and dark blue, respectively, substantially increased their $\Delta G_{reaction}$ values. We believe that these values correspond to their electron-donating or withdrawing capabilities. By supplying the ligand with electrons through electron donation and the sigma system, the lone pair on either the nitrogen or sulfur atom becomes more available. The opposite is true for electron-withdrawing groups.

This trend continues in Figures 22-24. The only difference is the methoxy group doesn't behave as expected. We believe the reasoning for this is strain which was mentioned in previous subsections. Methoxy is the only non-linear substituent and with the bulkiness of the methyl on the end of it can be difficult to work with.

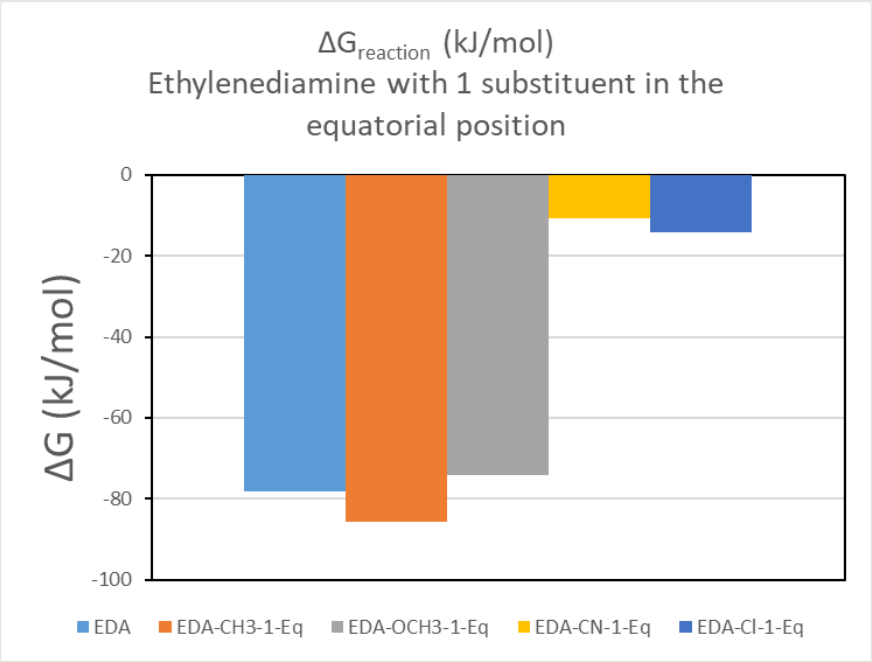

Figure 21. Ethylenediamine ΔG comparison between R=CH_3, OCH_3, CN, Cl

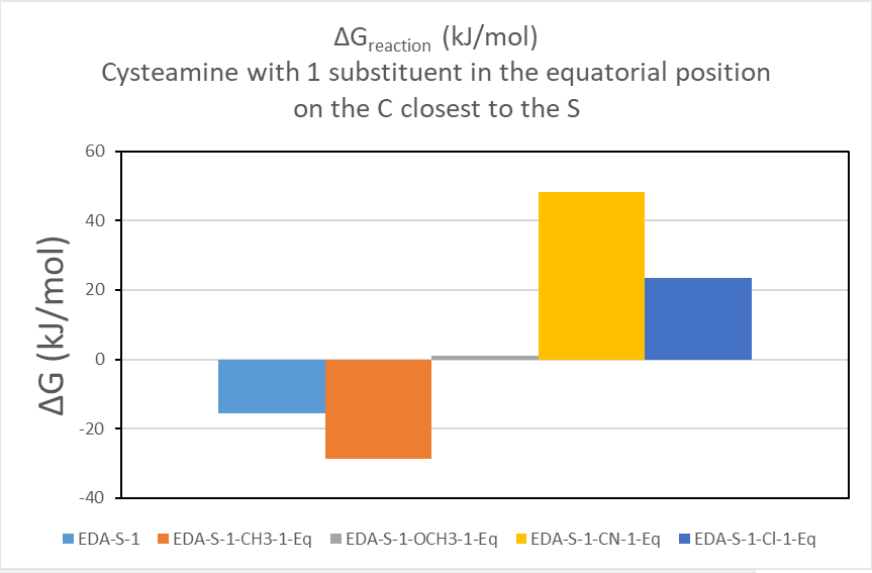

Figure 22. Cysteamine (sulfur) ΔG comparison between R=CH_3, OCH_3, CN, Cl

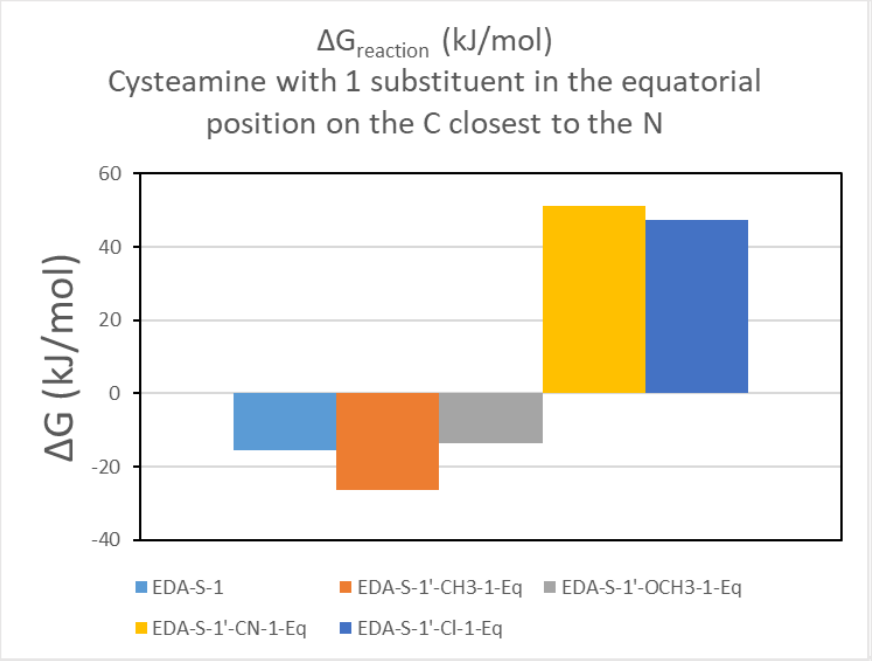

Figure 23. Cysteamine (nitrogen) ΔG comparison between R=CH_3, OCH_3, CN, Cl

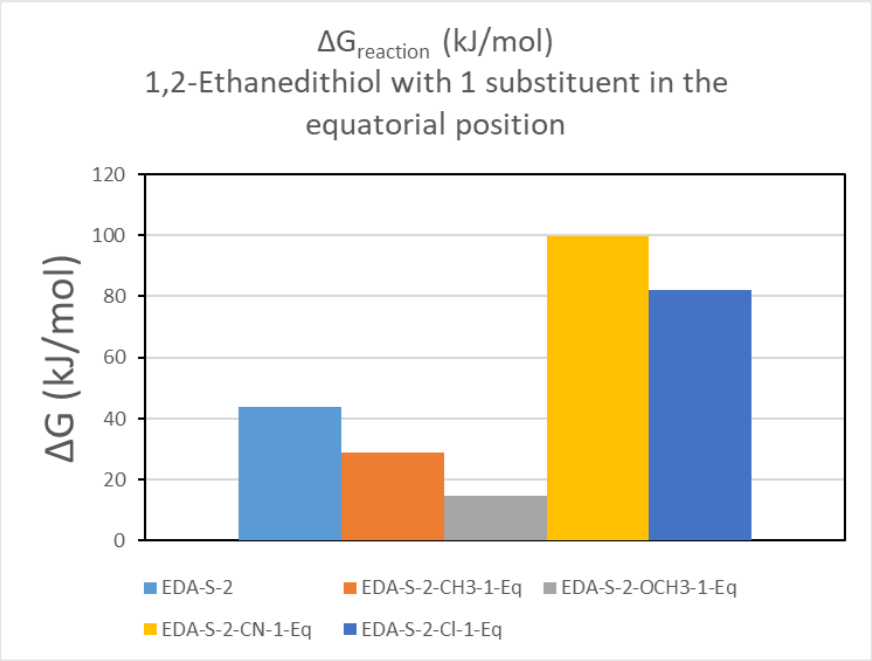

Figure 24. 1,2-Ethanedithiol ΔG comparison between R=CH_3, OCH_3, CN, Cl

3.5 Gibbs Free Energy, Enthalpy, & Entropy

Thermodynamic properties can tell us a great deal about the favorability of the reaction. Typically, $\Delta G_{reaction}$ is enough to understand the outcome of the reaction: entropy and enthalpy aren't talked about as much. Enthalpy ($\Delta H_{reaction}$) tells us whether a reaction is going to be endothermic or exothermic. If this value is negative, then the reaction will give off heat (exothermic). Entropy ($\Delta S_{reaction}$) tells us about disorder and order. When this value is positive, that means that the disorder of the reaction is growing and tends to be favorable. Finally, Energy ($\Delta G_{reaction}$) tells us about the spontaneity of reaction. The more negative this value is, the more spontaneous it is. That is to say, the more favorable it is. An unfavorable reaction would be positive. Because of the way the equation is written (Equation 8), whenever enthalpy is negative, and entropy is positive, our energy will always be negative[25].

Table 5 gives the $\Delta G_{reaction}$, $\Delta H_{reaction}$, and $\Delta S_{reaction}$ values for ethylenediamine complexes. It had the majority of the complexes having negative energy, which means that these reactions would be favorable. Most notably among them was ethylenediamine with a methoxy group in the axial position; it had a $\Delta G_{reaction}$ of almost -111 kJ/mol. This came as a surprise because we had expected the methyl group in the equatorial position to be the highest contender. This is because the methyl group has the highest electron-donating capabilities, and the equatorial position provides the most effect.

Tables 6-7 show the $\Delta G_{reaction}$, $\Delta H_{reaction}$, and $\Delta S_{reaction}$ for cysteamine and 1,2-ethanedithiol complexes, respectively. The cysteamine complexes had much higher values than the ethylenediamine complexes. This can only be attributed to the replacement of the nitrogen atom with sulfur. This trend continues with 1,2-ethanedithiol complexes (Table 7).

Additionally, it was observed that adding multiple substituents (in either the axial-equatorial or equatorial-equatorial positions) amplified the effect of just having one substituent. For example, in Table 6, when there is one methyl substituent in the equatorial position on the carbon closest to the sulfur atom (EDA-S-1-CH3-Eq) it has a $\Delta G_{reaction}$ value of -28.7 kJ/mol, but with an

additional methyl group in the equatorial position (EDA-S-1-CH3-Eq-Eq) that value decreases to -40.85 kJ/mol.

Table 5. $\Delta G_{reaction}$, $\Delta H_{reaction}$, and $\Delta S_{reaction}$ values for ethylenediamine (EDA) complexes

Name	Energy (kJ/mol)	Enthalpy (kJ/mol)	Entropy (kJ/mol)
EDA	-78.140131	-57.1702625	0.070333
EDA-CH3-1-Eq	-85.822344	-65.810783	0.067119
EDA-OCH3-1-Eq	-74.086359	-51.6409595	0.075282
EDA-CN-1-Eq	-10.7829285	9.472804	0.067938
EDA-Cl-1-Eq	-14.2590905	5.214243	0.065314
EDA-CH3-1-Ax	-84.131522	-64.0333195	0.06741
EDA-OCH3-1-Ax	-110.9457535	-91.383153	0.065613
EDA-CN-1-Ax	-10.953586	9.039596501	0.067057
EDA-Cl-1-Ax	-5.1801115	13.558082	0.062848
EDA-CH3-2-Ax-Eq	-92.1839305	-72.0515965	0.067524
EDA-OCH3-2-Ax-Eq	-76.155253	-52.5546335	0.079157
EDA-CN-2-Ax-Eq	31.590016	49.8608705	0.061281
EDA-Cl-2-Ax-Eq	42.517347	60.916851	0.061712
EDA-CH3-2-Eq-Eq	-98.797565	-76.6514725	0.074278
EDA-OCH3-2-Eq-Eq	-86.105898	-63.2614225	0.076621
EDA-CN-2-Eq-Eq	48.0597775	70.1402325	0.074058
EDA-Cl-2-Eq-Eq	38.789137	57.986793	0.064389

Table 6. $\Delta G_{reaction}$, $\Delta H_{reaction}$, and $\Delta S_{reaction}$ values for cysteamine (EDA-S-1) complexes

Name	Energy (kJ/mol)	Enthalpy (kJ/mol)	Entropy (kJ/mol)
EDA-S-1	-15.605972	3.7308355	0.064856
EDA-S-1-CH3-1-Eq	-28.7098425	-8.840058499	0.066644
EDA-S-1-OCH3-1-Eq	-37.539399	-17.7720095	0.0663
EDA-S-1-CN-1-Eq	48.1280405	68.1185975	0.067049
EDA-S-1-Cl-1-Eq	23.587492	42.69063	0.064072
EDA-S-1-CH3-1-Ax	-24.7243335	-6.322204	0.061721
EDA-S-1-OCH3-1-Ax	-40.9499235	-18.1238265	0.076559
EDA-S-1-CN-1-Ax	34.8850185	54.673412	0.066371
EDA-S-1-Cl-1-Ax	19.549473	39.156707	0.065763
EDA-S-1'-CH3-1-Eq	-26.2891315	-6.508614499	0.066344
EDA-S-1'-OCH3-1-Eq	-13.626345	8.9660825	0.075775
EDA-S-1'-CN-1-Eq	50.997712	70.368651	0.06497
EDA-S-1'-Cl-1-Eq	47.3193865	65.6033685	0.061325
EDA-S-1'-CH3-1-Ax	-22.784089	-3.486664	0.064724
EDA-S-1'-OCH3-1-Ax	-16.309606	-0.7272635	0.052263
EDA-S-1'-CN-1-Ax	36.268657	52.4128565	0.054148
EDA-S-1'-Cl-1-Ax	55.256273	74.474933	0.06446
EDA-S-1-CH3-2-Ax-Eq	-35.055676	-16.309606	0.062875
EDA-S-1-OCH3-2-Ax-Eq	-41.0601945	-15.548211	0.085568
EDA-S-1-CN-2-Ax-Eq	92.8455565	113.327082	0.068695
EDA-S-1-Cl-2-Ax-Eq	71.838931	91.204619	0.064953
EDA-S-1-CH3-2-Eq-Eq	-40.8501545	-19.5941065	0.071293
EDA-S-1-OCH3-2-Eq-Eq	-41.551163	-20.42639	0.070853
EDA-S-1-CN-2-Eq-Eq	105.6317415	126.060757	0.068519
EDA-S-1-Cl-2-Eq-Eq	71.78117	91.677209	0.066732

Table 7. $\Delta G_{reaction}$, $\Delta H_{reaction}$, and $\Delta S_{reaction}$ values for 1,2-ethanedithiol (EDA-S-2) complexes

Name	Energy (kJ/mol)	Enthalpy (kJ/mol)	Entropy (kJ/mol)
EDA-S-2	43.7172005	61.483959	0.05959
EDA-S-2-CH3-1-Eq	28.822739	47.5714345	0.062883
EDA-S-2-OCH3-1-Eq	14.781565	35.1475685	0.068308
EDA-S-2-CN-1-Eq	99.7401195	118.315532	0.062302
EDA-S-2-Cl-1-Eq	82.2857955	101.3311725	0.063879
EDA-S-2-CH3-1-Ax	30.224756	49.532683	0.064759
EDA-S-2-OCH3-1-Ax	20.5917965	40.7503855	0.067612
EDA-S-2-CN-1-Ax	83.522406	101.486077	0.06025
EDA-S-2-Cl-1-Ax	71.6577715	91.099599	0.065208
EDA-S-2-CH3-2-Ax-Eq	18.042436	36.541709	0.062047
EDA-S-2-OCH3-2-Ax-Eq	0.6064905	25.173294	0.082397
EDA-S-2-CN-2-Ax-Eq	134.194556	152.903869	0.062751
EDA-S-2-Cl-2-Ax-Eq	125.745697	121.2167095	-0.01519
EDA-S-2-CH3-2-Eq-Eq	12.481627	32.81875	0.068211
EDA-S-2-OCH3-2-Eq-Eq	12.4527465	36.9381595	0.082124
EDA-S-2-CN-2-Eq-Eq	148.104455	168.5649765	0.068625
EDA-S-2-Cl-2-Eq-Eq	102.8224565	124.033871	0.071143

3.6 Gibb's Free Energy v. Bond Distance Correlation

Energy and bond distance were found to be closely related in all cases. There was a single outlier found in the cysteamine complexes. This was EDA-S-1-N-OCH3-AX (Figure 61). It was observed that the oxygen atom on the methoxy substituent encroached closely to the uranium center. This crowding is typical of pushing the metal-ligand bond further away and is the cause for such a high bond distance.

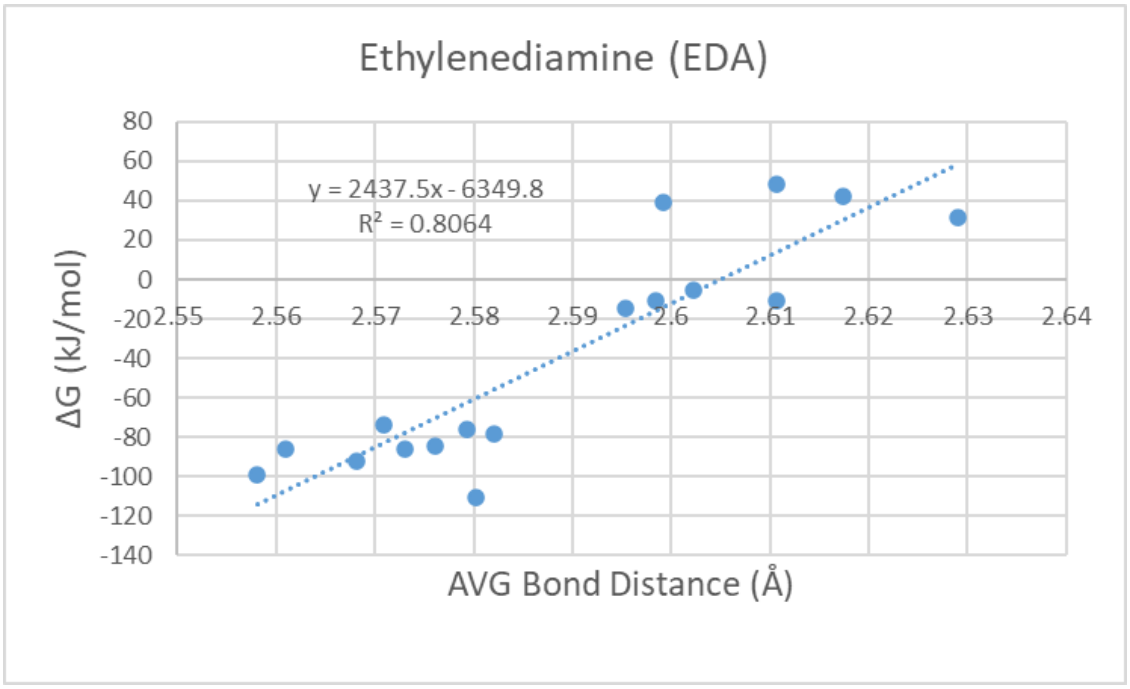

Figure 25. Ethylenediamine (EDA) Gibb's free energy of the reaction and bond distance relation

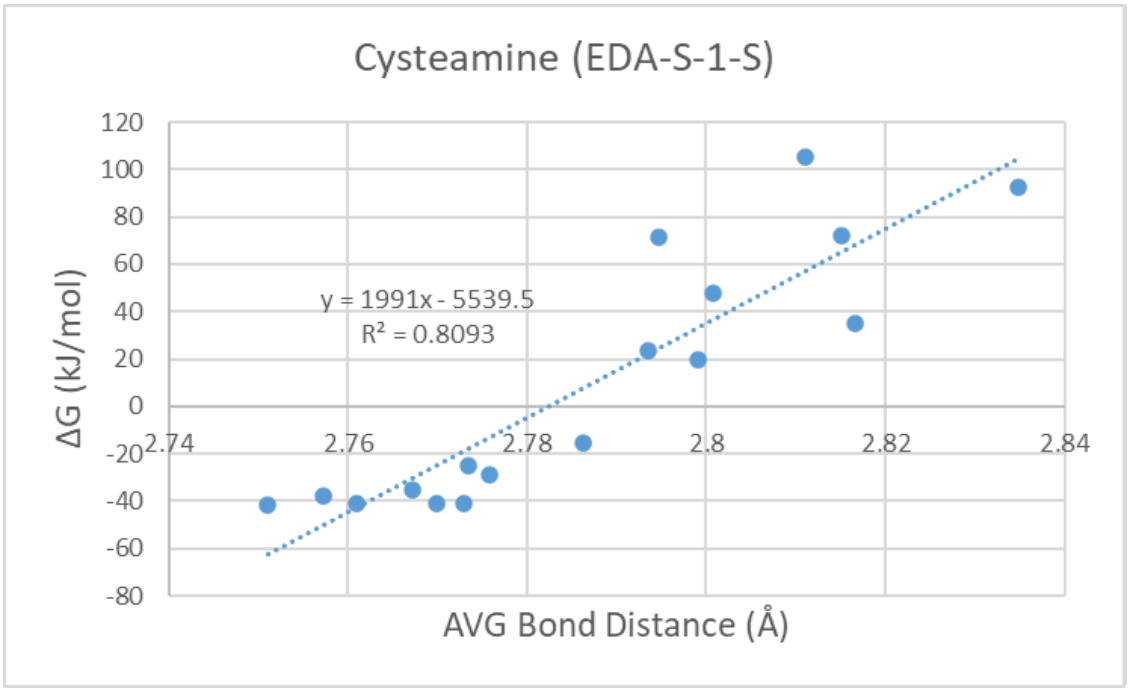

Figure 26. Cysteamine (EDA-S-1-S) Gibb's free energy of the reaction and bond distance relation

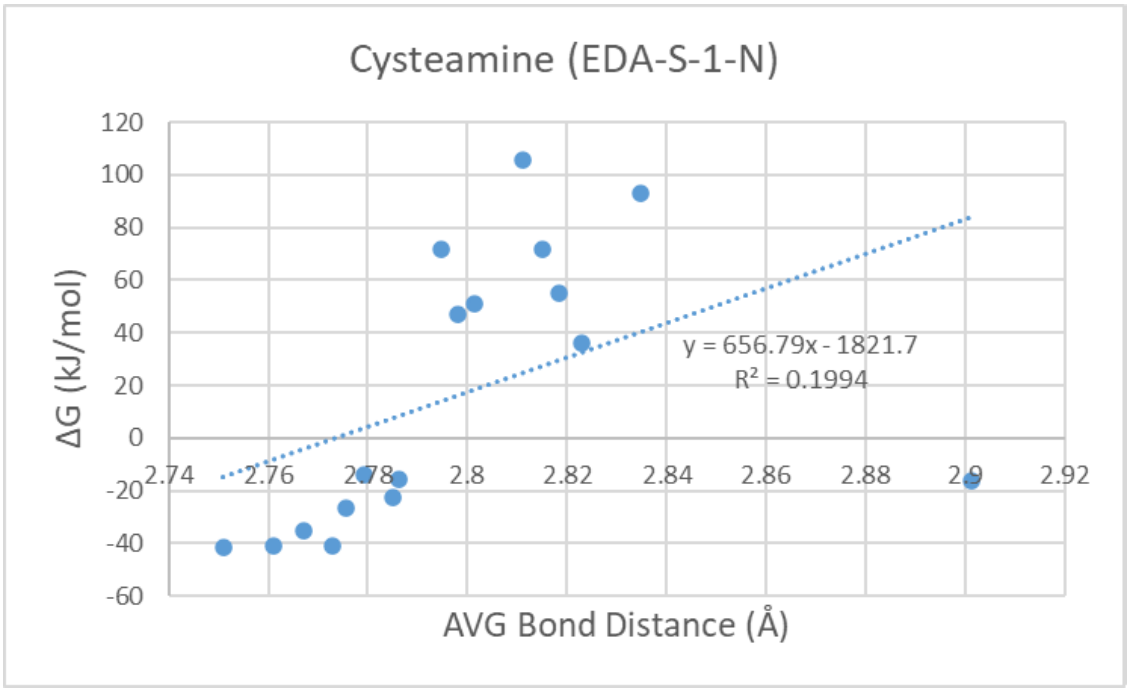

Figure 27. Cysteamine (EDA-S-1-N) Gibb's free energy of the reaction and bond distance relation

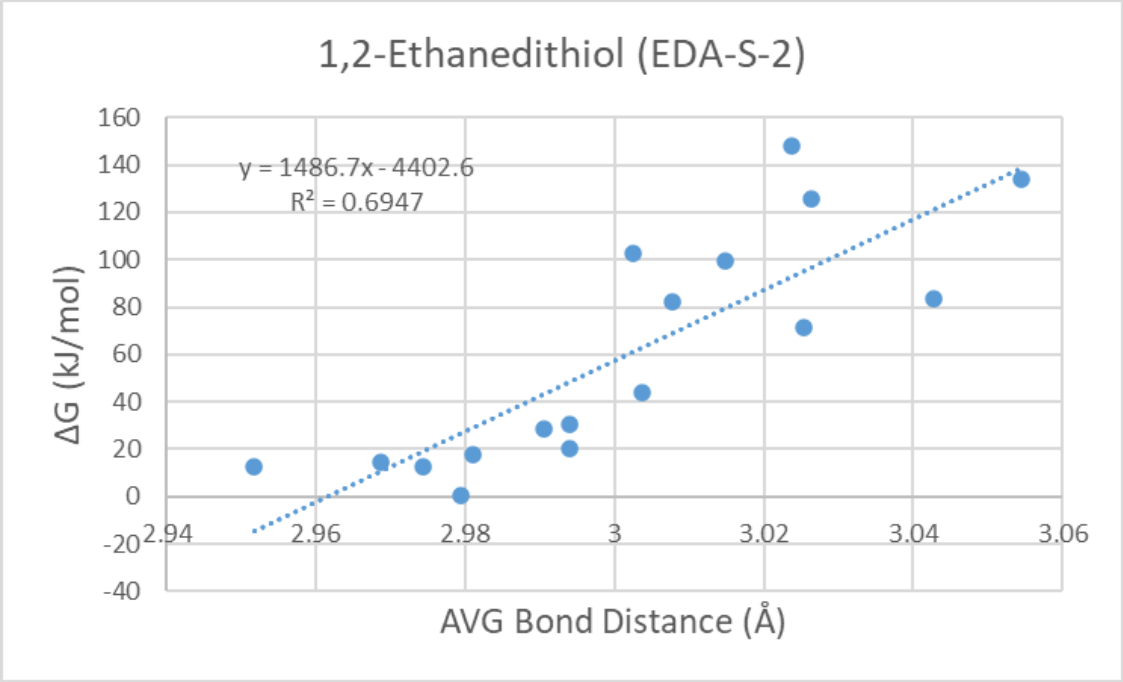

Figure 28. 1,2-Ethanedithiol (EDA-S-2) Gibb's free energy of the reaction and bond distance relation

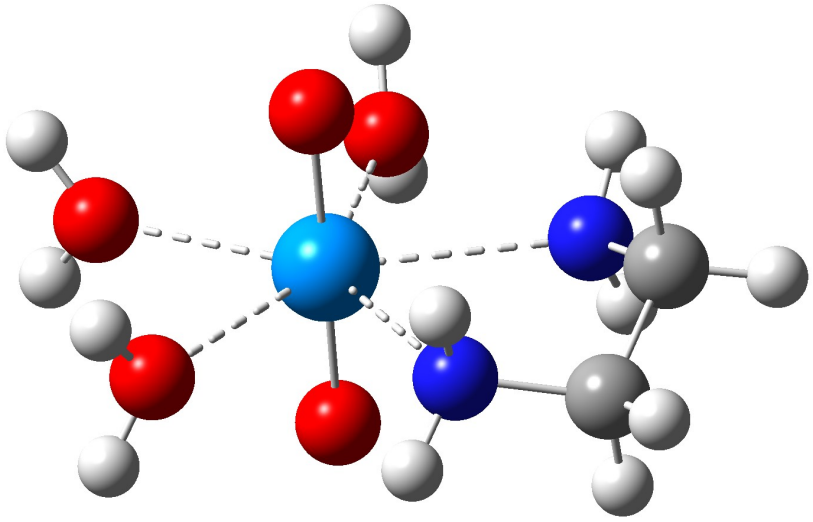

Figure 29. Ethylenediamine (EDA)

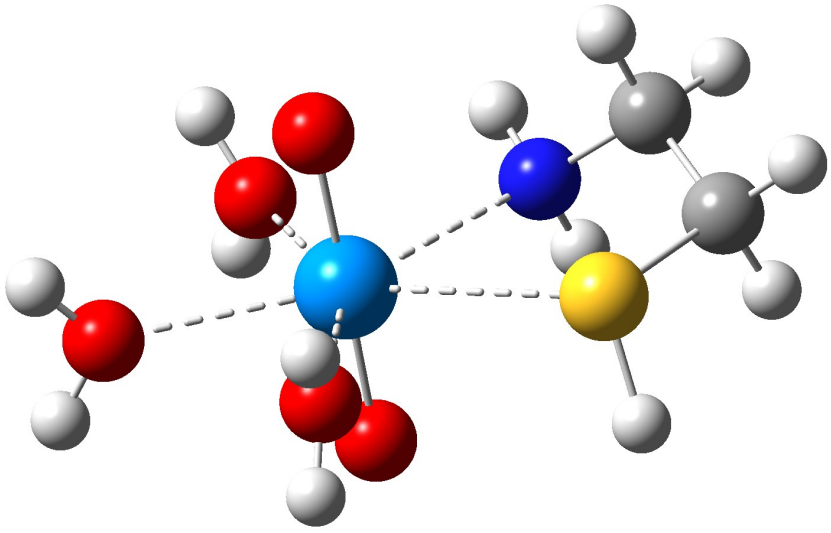

Figure 30. Cysteamine (EDA-S-1)

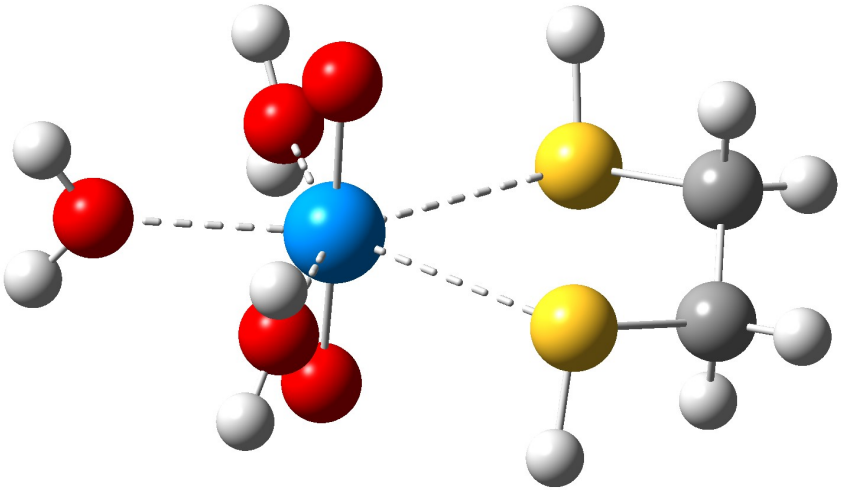

Figure 31. 1,2-Ethanedithiol (EDA-S-2)

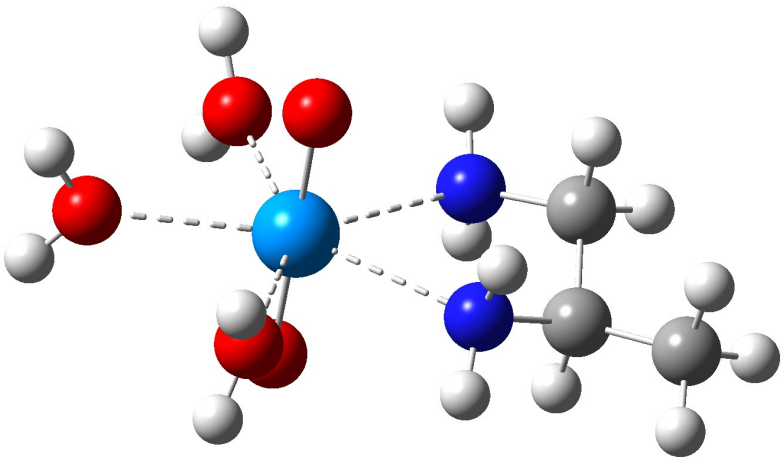

Figure 32. Ethylenediamine with methyl in the equatorial position (EDA-CH3-EQ)

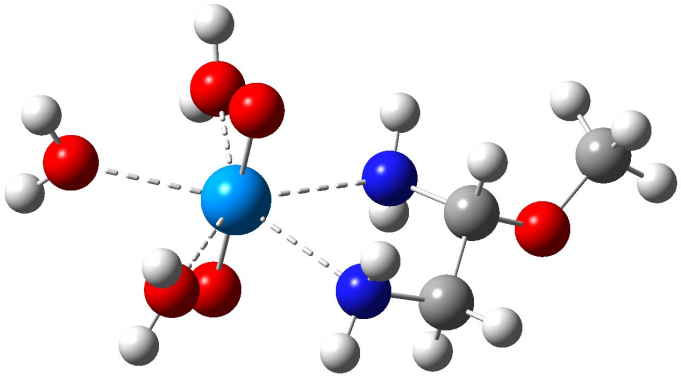

Figure 33. Ethylenediamine with methoxy in the equatorial position (EDA-OCH3-EQ)

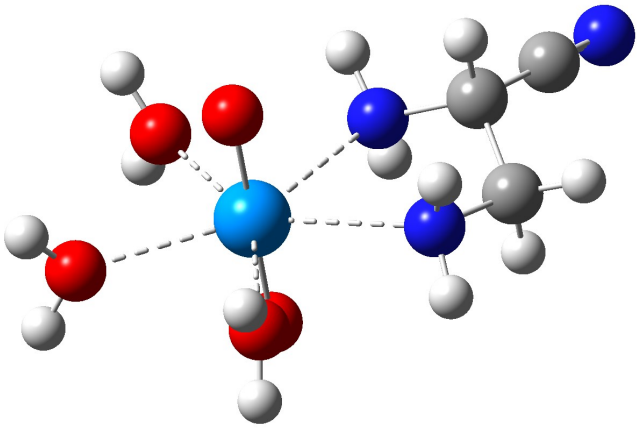

Figure 34. Ethylenediamine with cyanide in the equatorial position (EDA-CN-EQ)

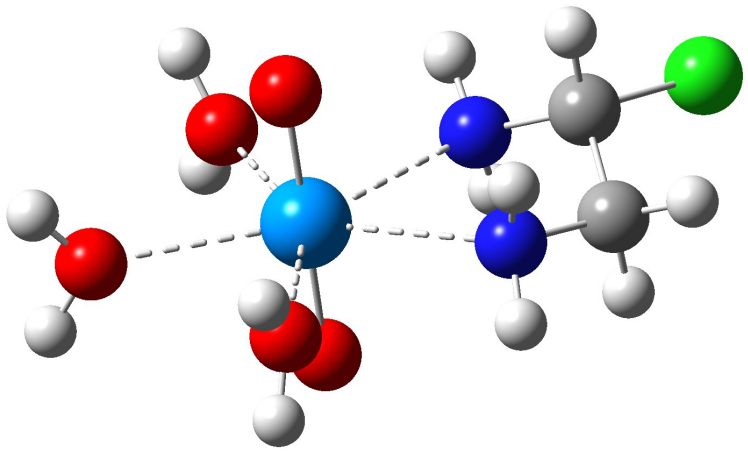

Figure 35. Ethylenediamine with chlorine in the equatorial position (EDA-Cl-EQ)

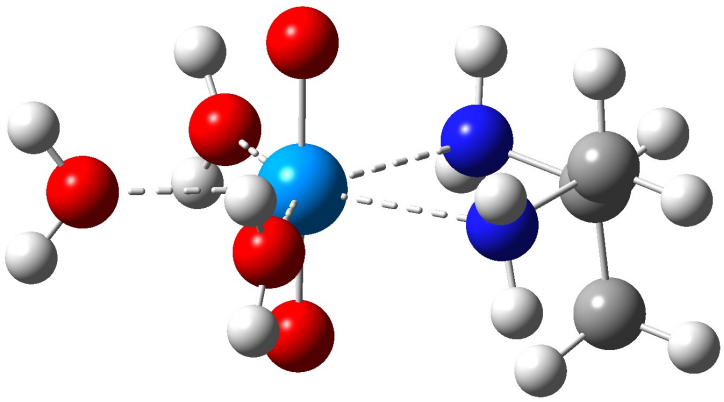

Figure 36. Ethylenediamine with methyl in the axial position (EDA-CH3-AX)

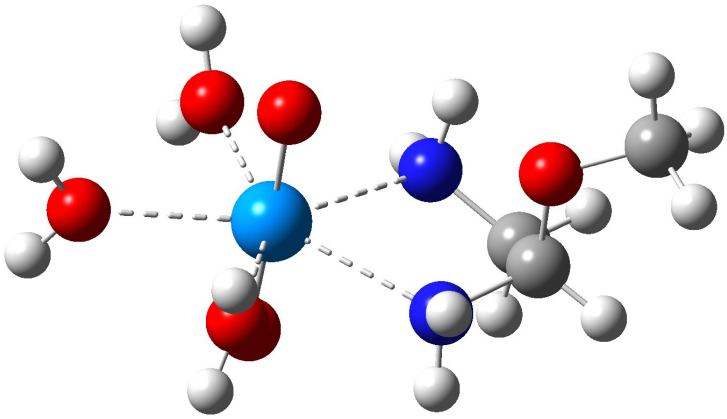

Figure 37. Ethylenediamine with methoxy in the axial position (EDA-OCH3-AX)

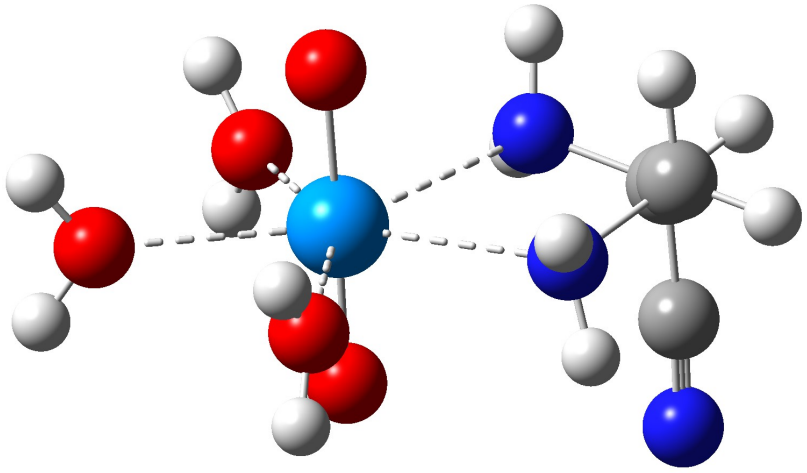

Figure 38. Ethylenediamine with cyanide in the axial position (EDA-CN-AX)

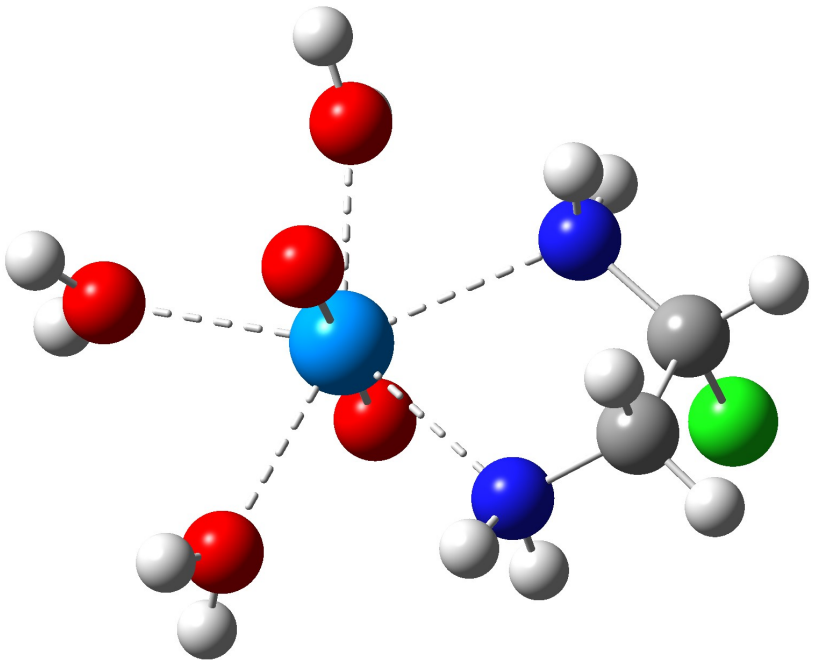

Figure 39. Ethylenediamine with chlorine in the axial position (EDA-Cl-AX)

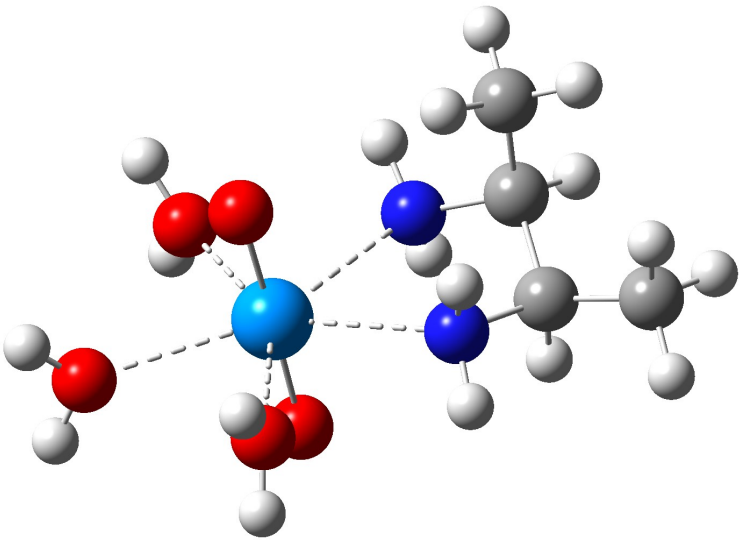

Figure 40. Ethylenediamine with two methyl groups in the axial-equatorial position (EDA-CH3-2-AXEQ)

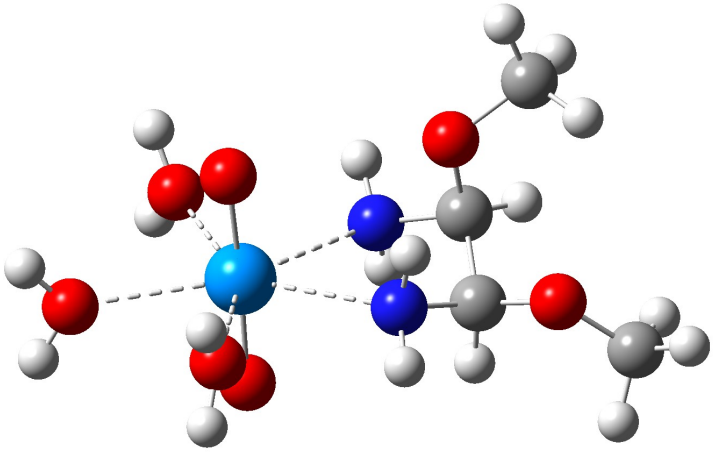

Figure 41. Ethylenediamine with two methoxy groups in the axial-equatorial position (EDA-OCH3-2-AXEQ)

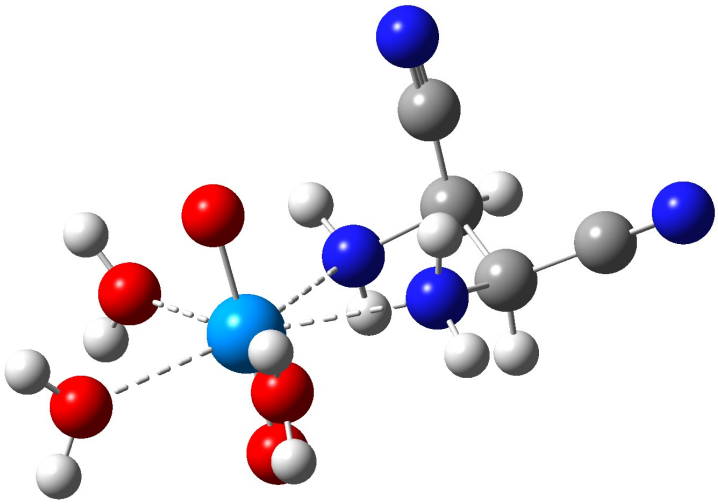

Figure 42. Ethylenediamine with two cyanide groups in the axial-equatorial position (EDA-CN-2-AXEQ)

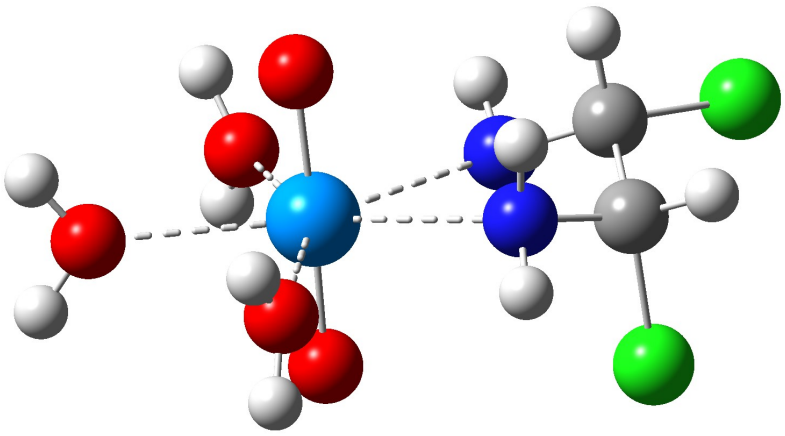

Figure 43. Ethylenediamine with two chlorine groups in the axial-equatorial position (EDA-Cl-2-AXEQ)

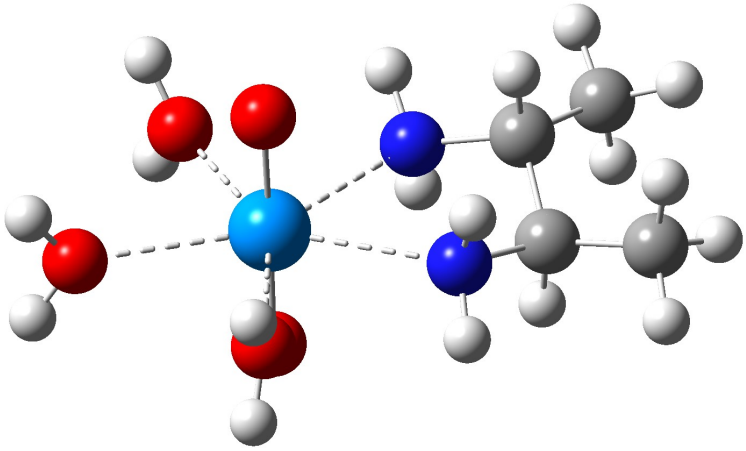

Figure 44. Ethylenediamine with two methyl groups in the equatorial position (EDA-CH3-2-EQEQ)

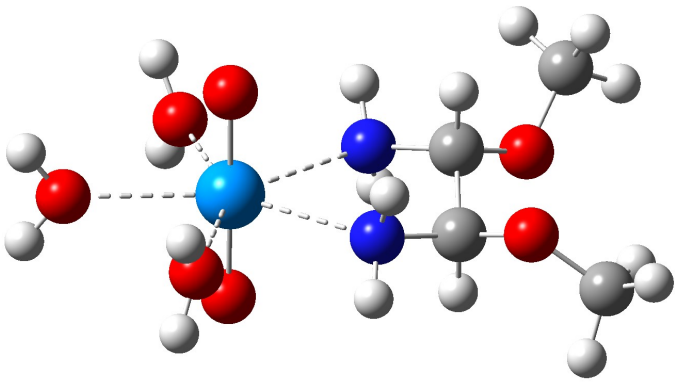

Figure 45. Ethylenediamine with two methoxy groups in the equatorial position (EDA-OCH3-2-EQEQ)

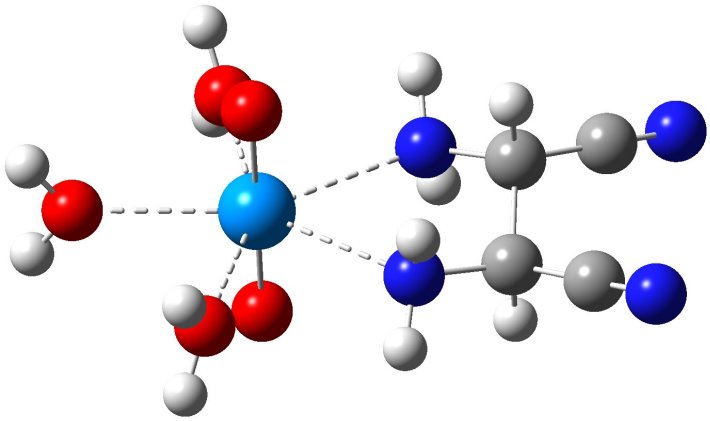

Figure 46. Ethylenediamine with two cyanide groups in the equatorial position (EDA-CN-2-EQEQ)

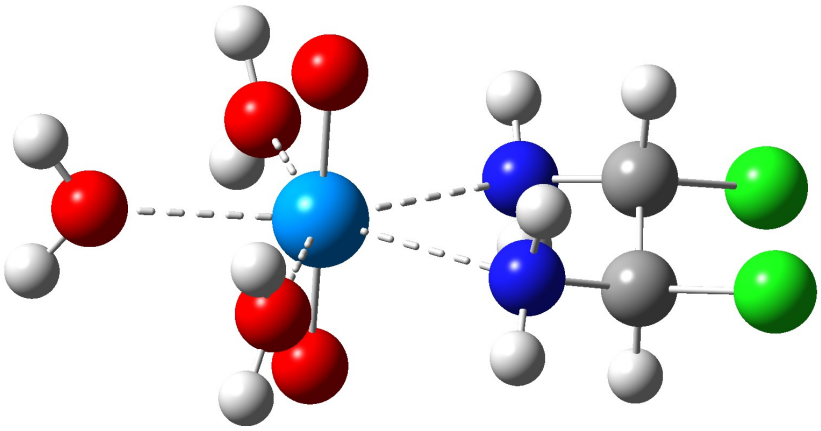

Figure 47. Ethylenediamine with two chlorine groups in the equatorial position (EDA-Cl-2-EQEQ)

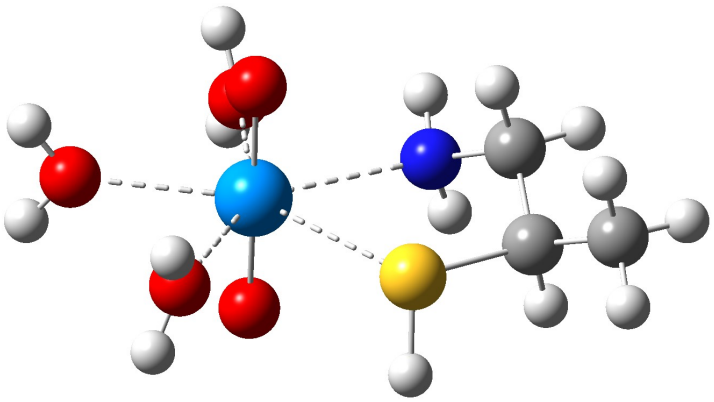

Figure 48. Cysteamine with a methyl group attached to the carbon closest to the sulfur in the equatorial position (EDA-S-1-S-CH3-EQ)

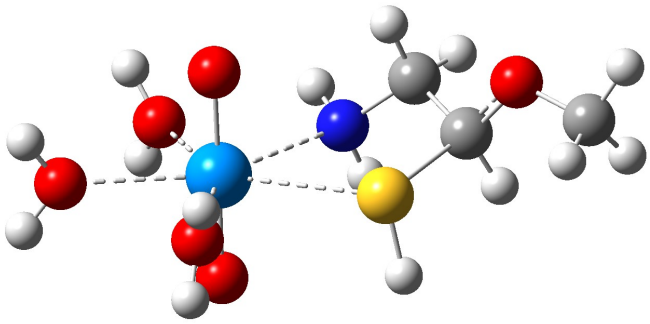

Figure 49. Cysteamine with a methoxy group attached to the carbon closest to the sulfur in the equatorial position (EDA-S-1-S-OCH3-EQ)

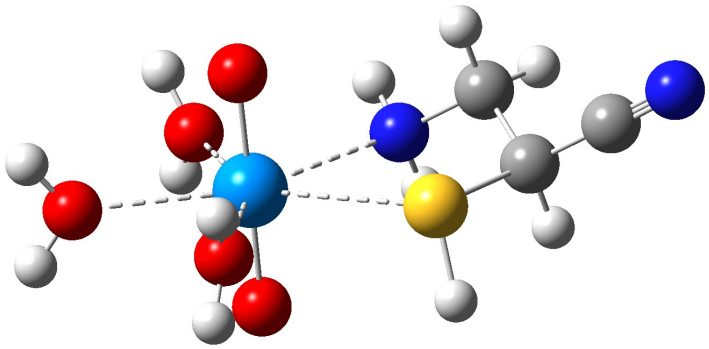

Figure 50. Cysteamine with a cyanide group attached to the carbon closest to the sulfur in the equatorial position (EDA-S-1-S-CN-EQ)

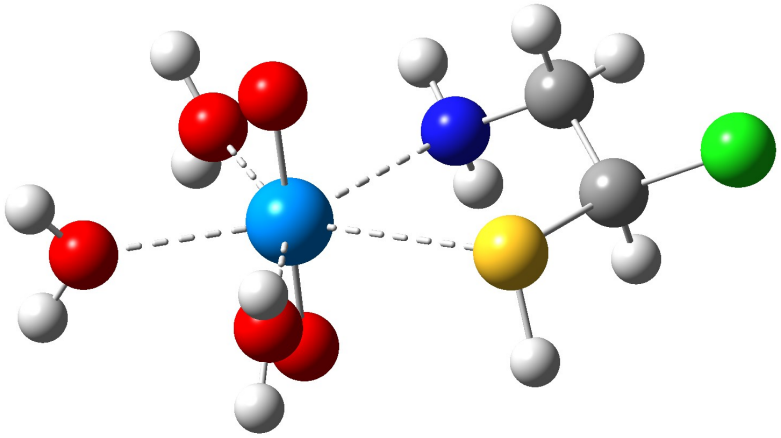

Figure 51. Cysteamine with a chlorine group attached to the carbon closest to the sulfur in the equatorial position (EDA-S-1-S-Cl-EQ)

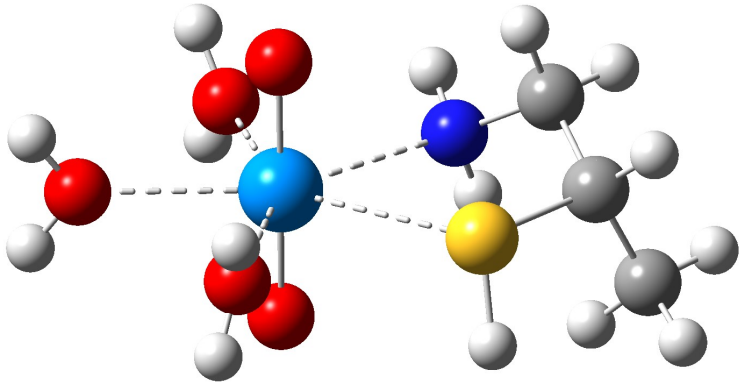

Figure 52. Cysteamine with a methyl group attached to the carbon closest to the sulfur in the axial position (EDA-S-1-S-CH3-AX)

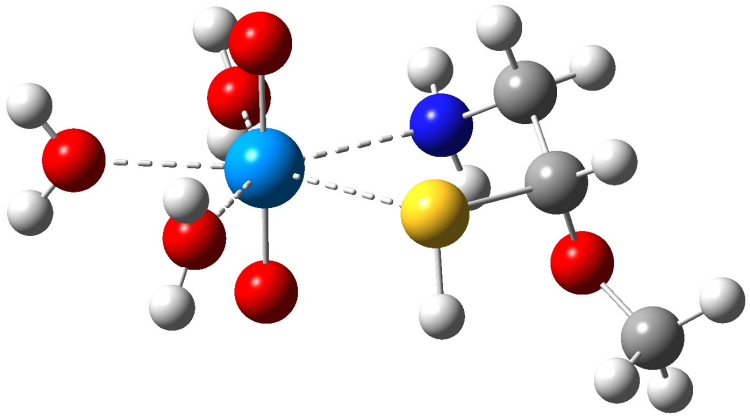

Figure 53. Cysteamine with a methoxy group attached to the carbon closest to the sulfur in the axial position (EDA-S-1-S-OCH3-AX)

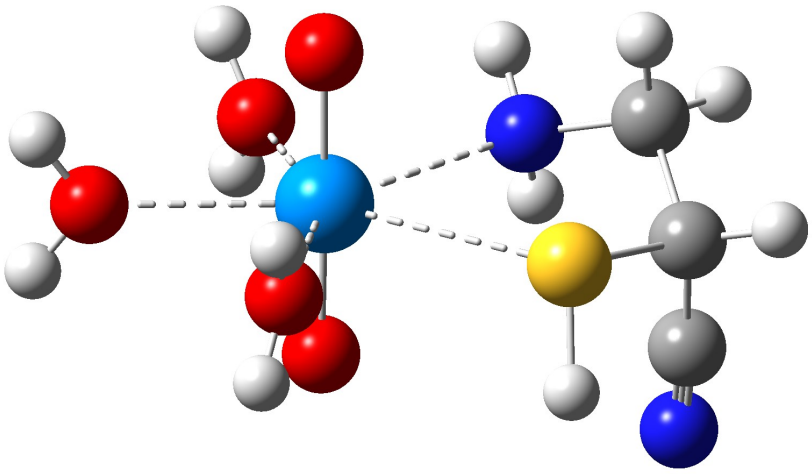

Figure 54. Cysteamine with a cyanide group attached to the carbon closest to the sulfur in the axial position (EDA-S-1-S-CN-AX)

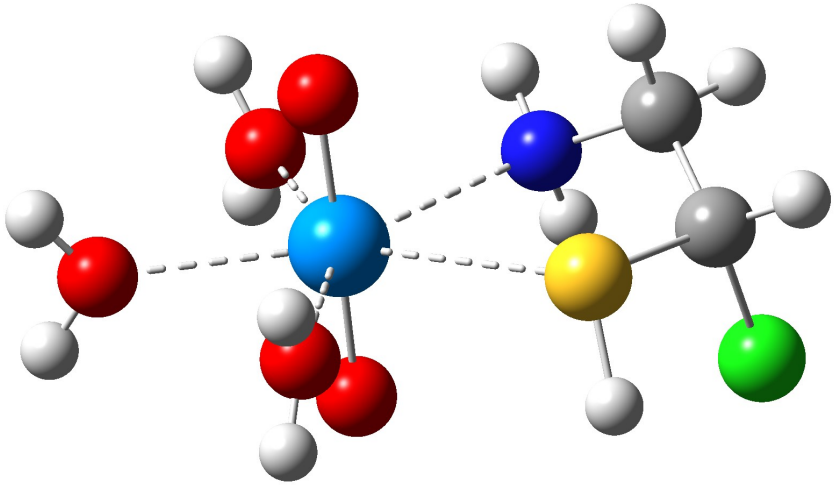

Figure 55. Cysteamine with a chlorine group attached to the carbon closest to the sulfur in the axial position (EDA-S-1-S-Cl-AX)

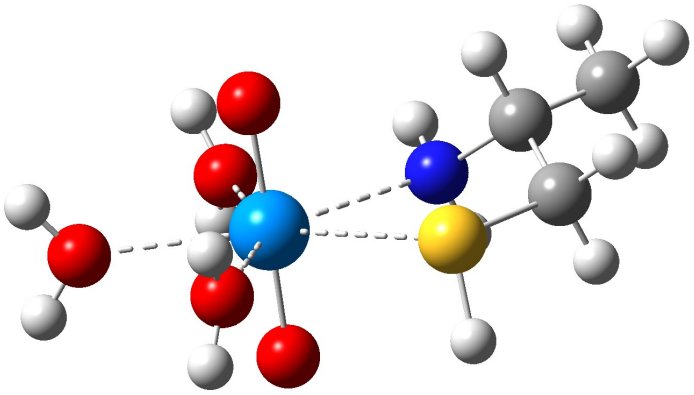

Figure 56. Cysteamine with a methyl group attached to the carbon closest to the nitrogen in the equatorial position (EDA-S-1-N-CH3-EQ)

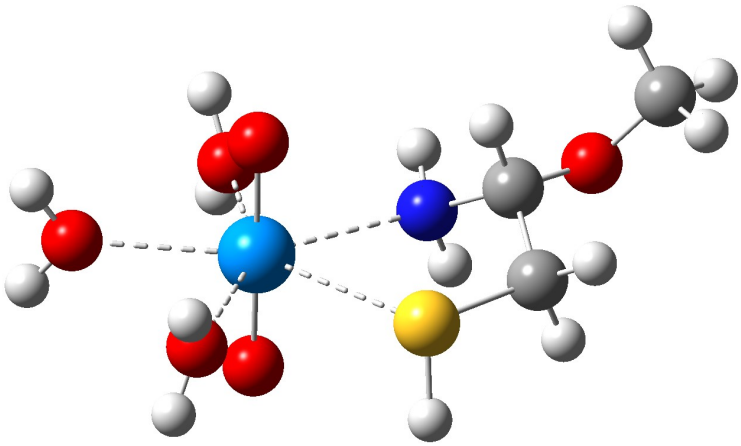

Figure 57. Cysteamine with a methoxy group attached to the carbon closest to the nitrogen in the equatorial position (EDA-S-1-N-OCH3-EQ)

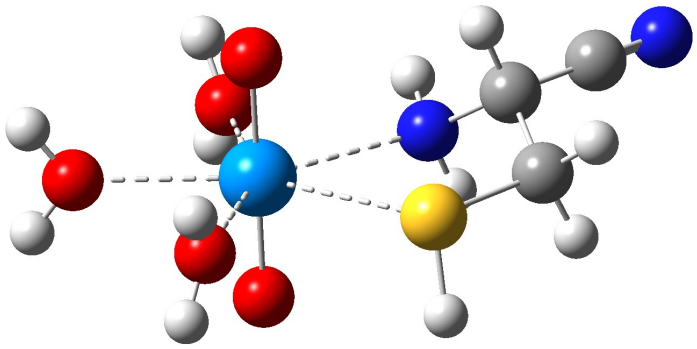

Figure 58. Cysteamine with a cyanide group attached to the carbon closest to the nitrogen in the equatorial position (EDA-S-1-N-CN-EQ)

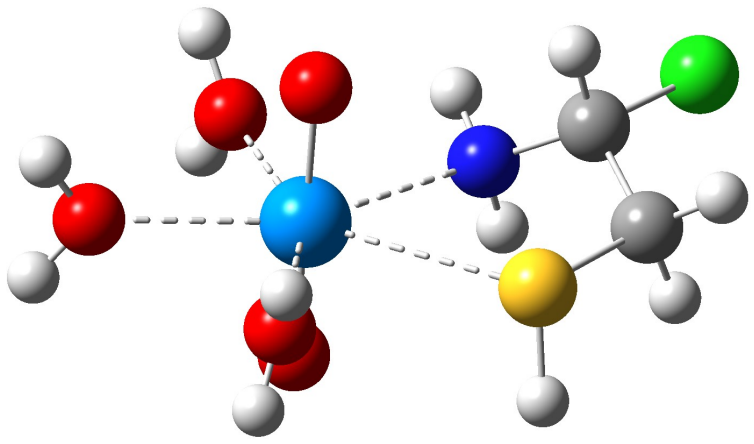

Figure 59. Cysteamine with a chlorine group attached to the carbon closest to the nitrogen in the equatorial position (EDA-S-1-N-Cl-EQ)

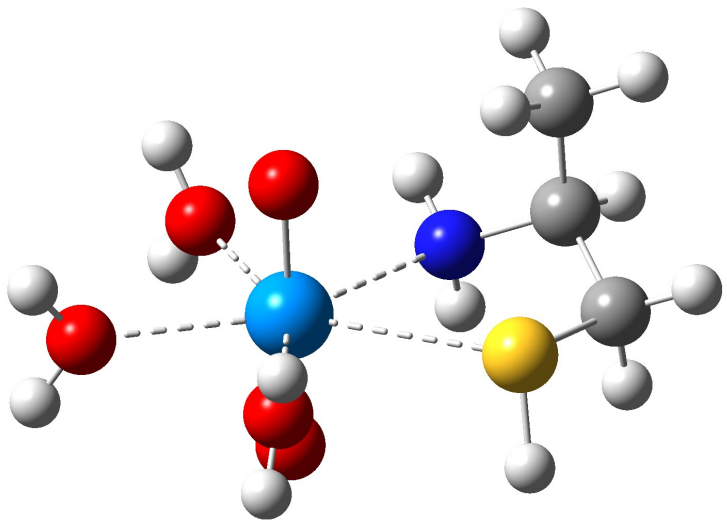

Figure 60. Cysteamine with a methyl group attached to the carbon closest to the nitrogen in the axial position (EDA-S-1-N-CH3-AX)

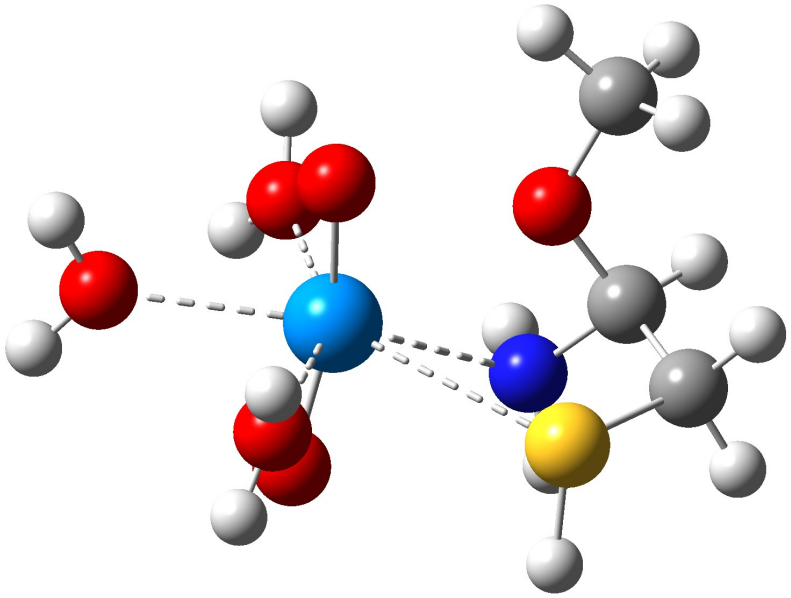

Figure 61. Cysteamine with a methoxy group attached to the carbon closest to the nitrogen in the axial position (EDA-S-1-N-OCH3-AX)

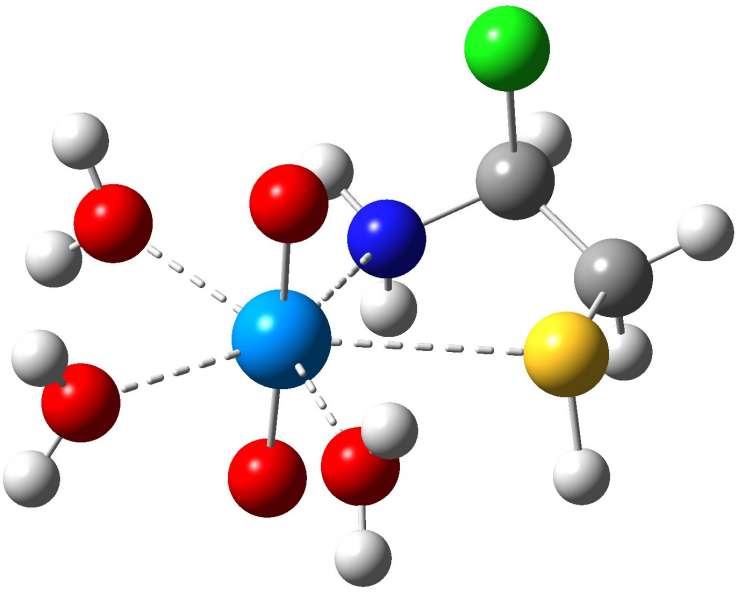

Figure 62. Cysteamine with a chlorine group attached to the carbon closest to the nitrogen in the axial position (EDA-S-1-N-Cl-AX)

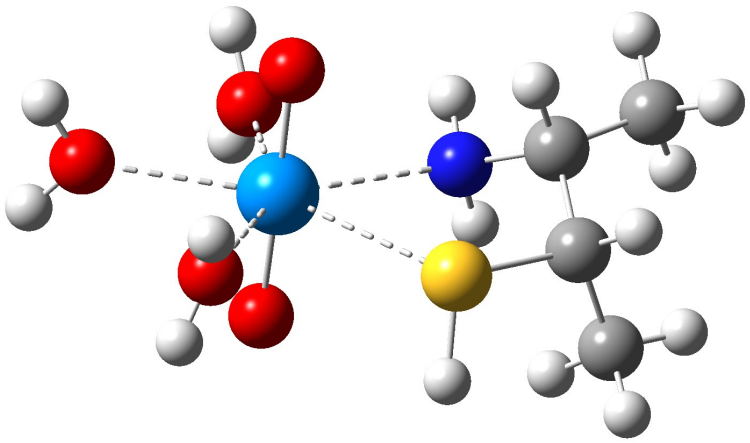

Figure 63. Cysteamine with two methyl groups attached in the axial-equatorial position (EDA-S-1-CH3-2-AXEQ)

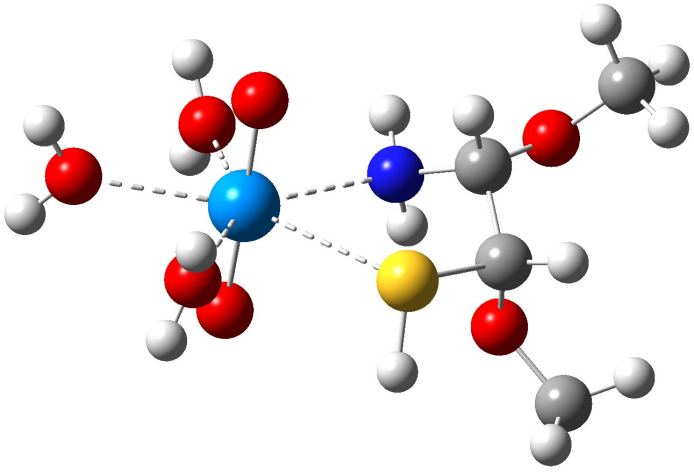

Figure 64. Cysteamine with two methoxy groups attached in the axial-equatorial position (EDA-S-1-OCH3-2-AXEQ)

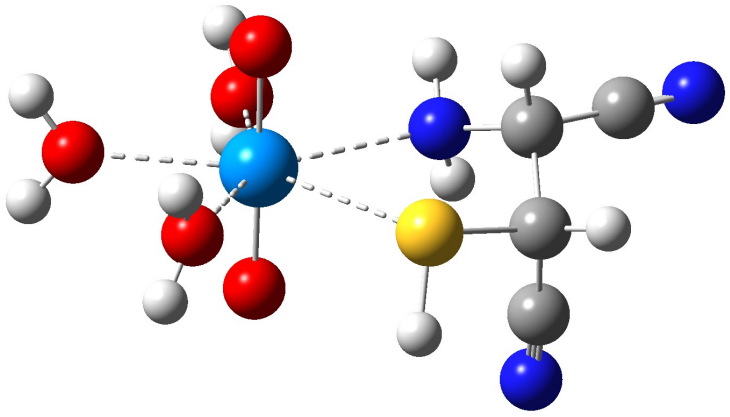

Figure 65. Cysteamine with two cyanide groups attached in the axial-equatorial position (EDA-S-1-CN-2-AXEQ)

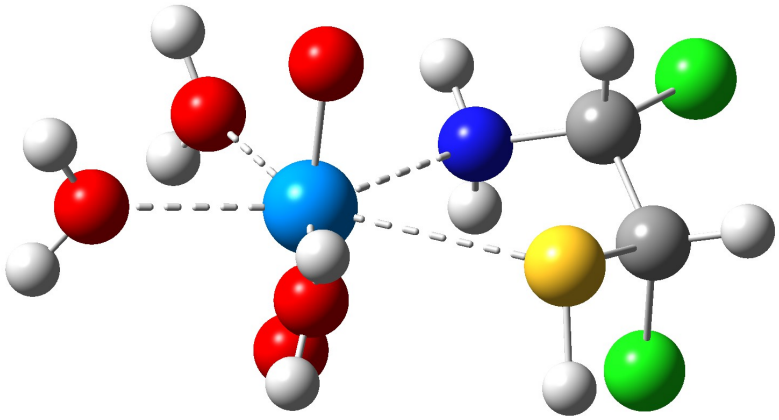

Figure 66. Cysteamine with two chlorine groups attached in the axial-equatorial position (EDA-S-1-Cl-2-AXEQ)

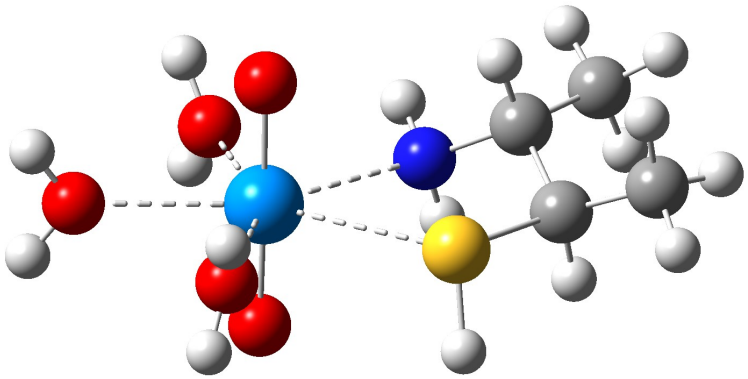

Figure 67. Cysteamine with two methyl groups attached in the equatorial-equatorial position (EDA-S-1-CH3-2-EQEQ)

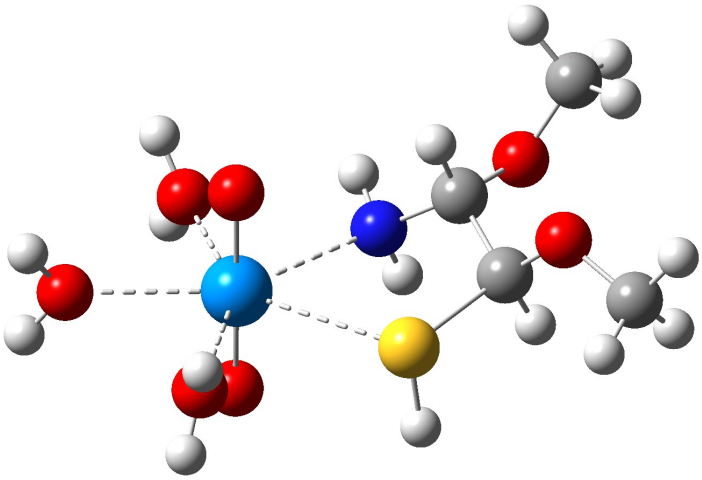

Figure 68. Cysteamine with two methoxy groups attached in the equatorial-equatorial position (EDA-S-1-OCH3-2-EQEQ)

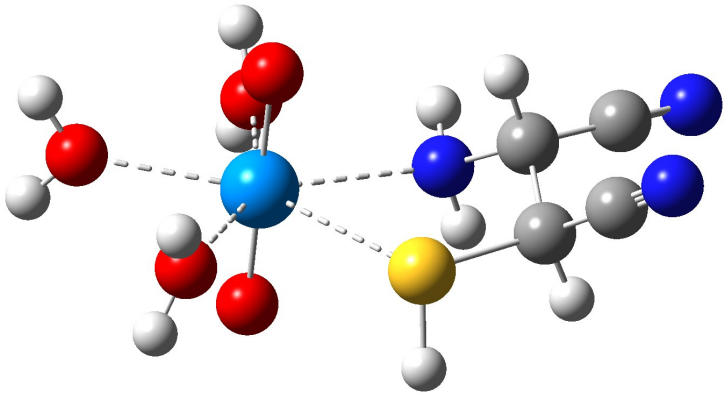

Figure 69. Cysteamine with two cyanide groups attached in the equatorial-equatorial position (EDA-S-1-CN-2-EQEQ)

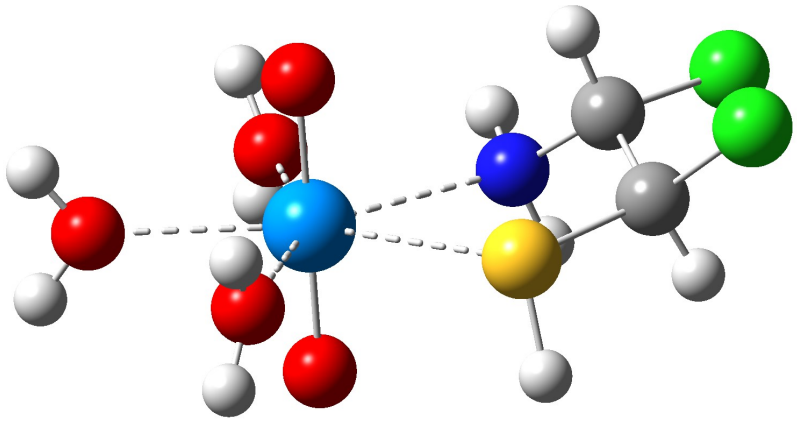

Figure 70. Cysteamine with two chlorine groups attached in the equatorial-equatorial position (EDA-S-1-Cl-2-EQEQ)

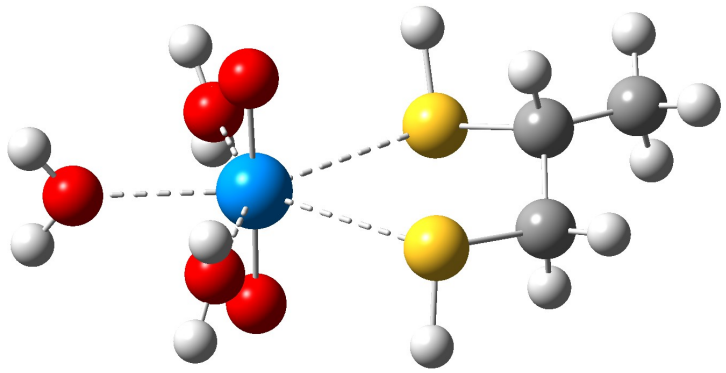

Figure 71. 1,2-Ethanedithiol with methyl in the equatorial position (EDA-S-2-CH3-EQ)

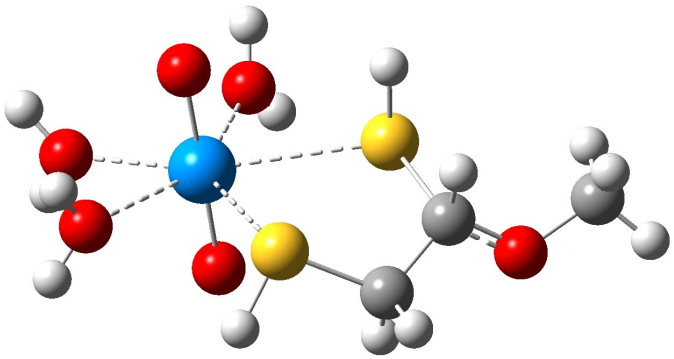

Figure 72. 1,2-Ethanedithiol with methoxy in the equatorial position (EDA-S-2-OCH3-EQ)

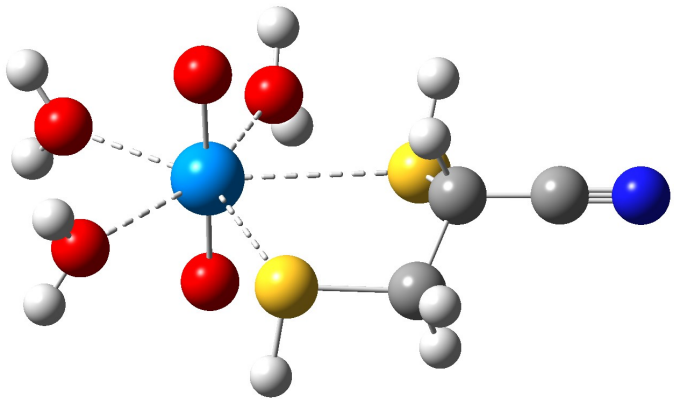

Figure 73. 1,2-Ethanedithiol with cyanide in the equatorial position (EDA-S-2-CN-EQ)

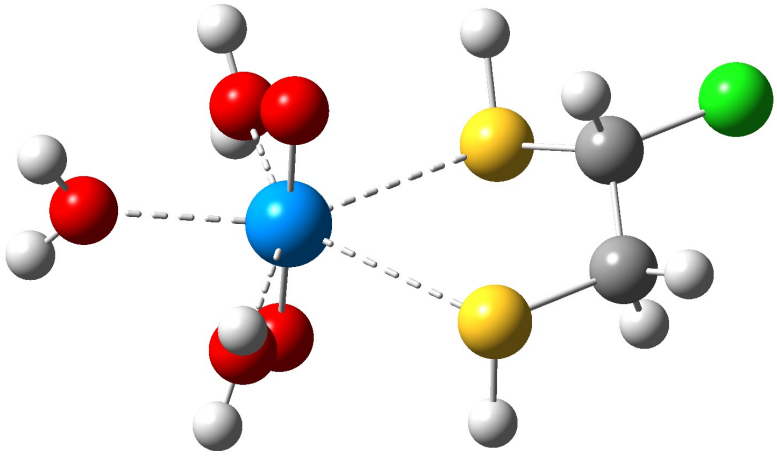

Figure 74. 1,2-Ethanedithiol with chlorine in the equatorial position (EDA-S-2-Cl-EQ)

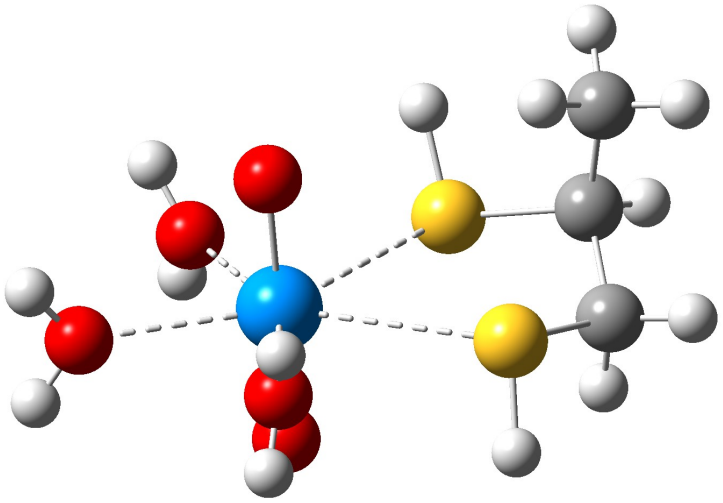

Figure 75. 1,2-Ethanedithiol with methyl in the axial position (EDA-S-2-CH3-AX)

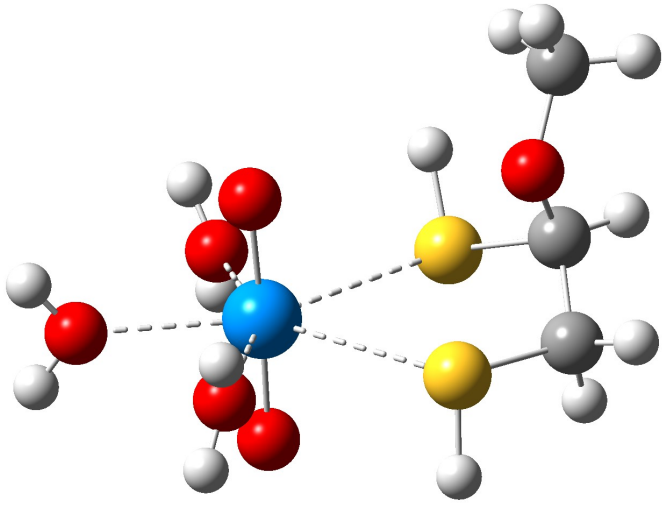

Figure 76. 1,2-Ethanedithiol with methoxy in the axial position (EDA-S-2-OCH3-AX)

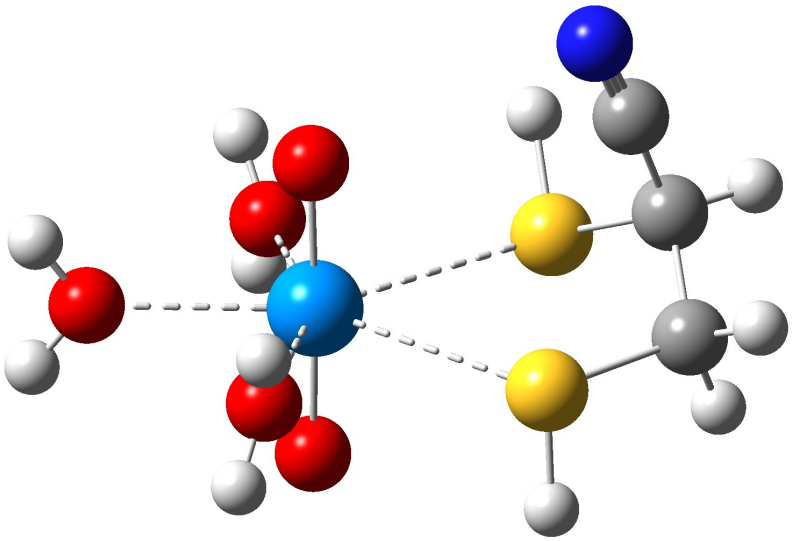

Figure 77. 1,2-Ethanedithiol with cyanide in the axial position (EDA-S-2-CN-AX)

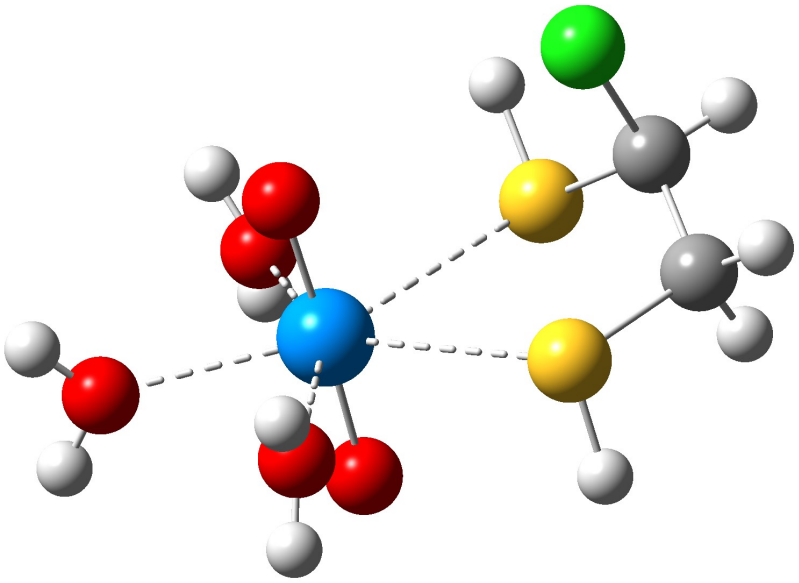

Figure 78. 1,2-Ethanedithiol with chlorine in the axial position (EDA-S-2-Cl-AX)

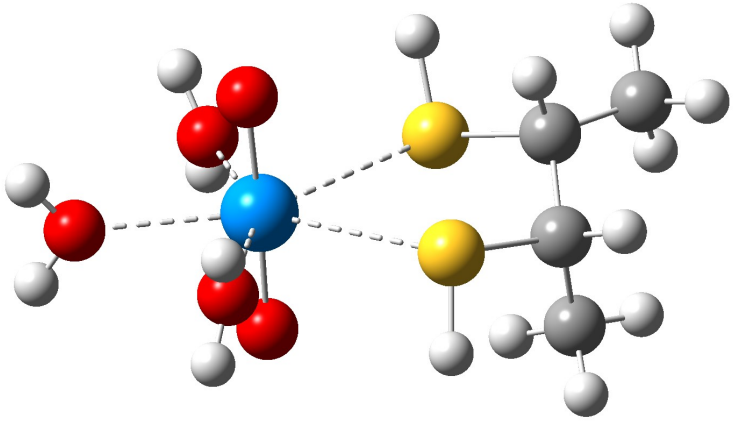

Figure 79. 1,2-Ethanedithiol with two methyl groups in the axial-equatorial position (EDA-S-2-CH3-2-AXEQ)

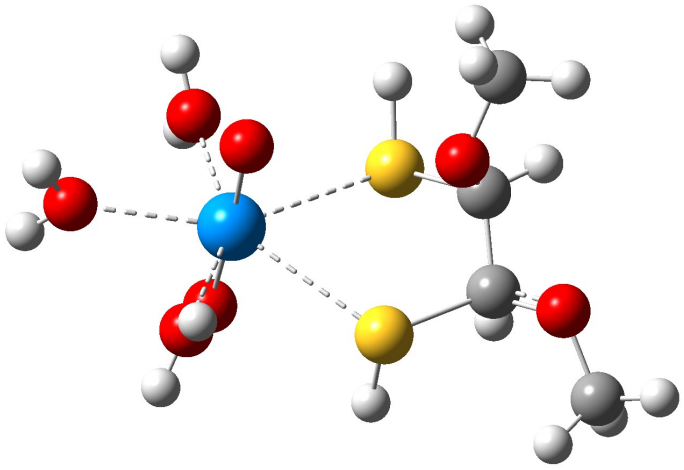

Figure 80. 1,2-Ethanedithiol with two methoxy groups in the axial-equatorial position (EDA-S-2-OCH3-2-AXEQ)

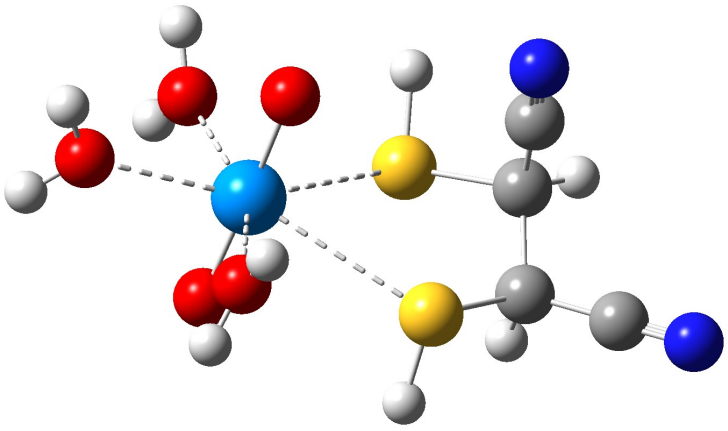

Figure 81. 1,2-Ethanedithiol with two cyanide groups in the axial-equatorial position (EDA-S-2-CN-2-AXEQ)

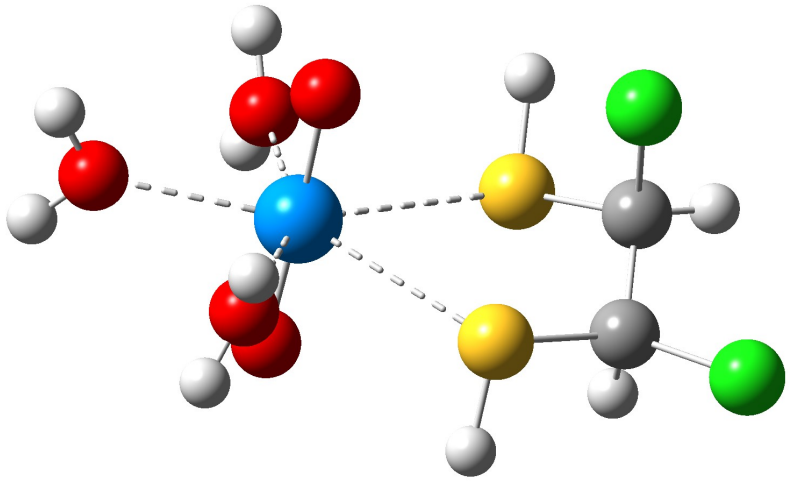

Figure 82. 1,2-Ethanedithiol with two chlorine groups in the axial-equatorial position (EDA-S-2-Cl-2-AXEQ)

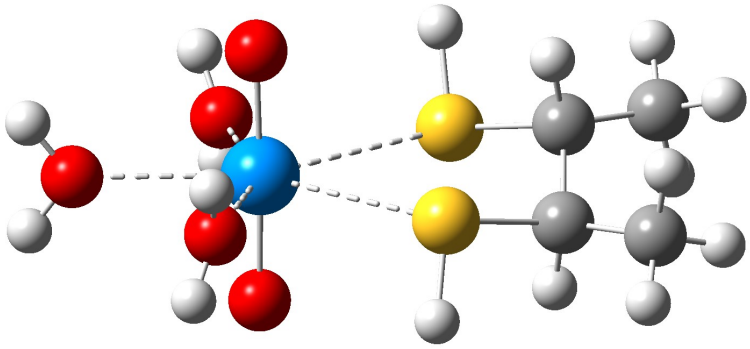

Figure 83. 1,2-Ethanedithiol with two methyl groups in the equatorial-equatorial position (EDA-S-2-CH3-2-EQEQ)

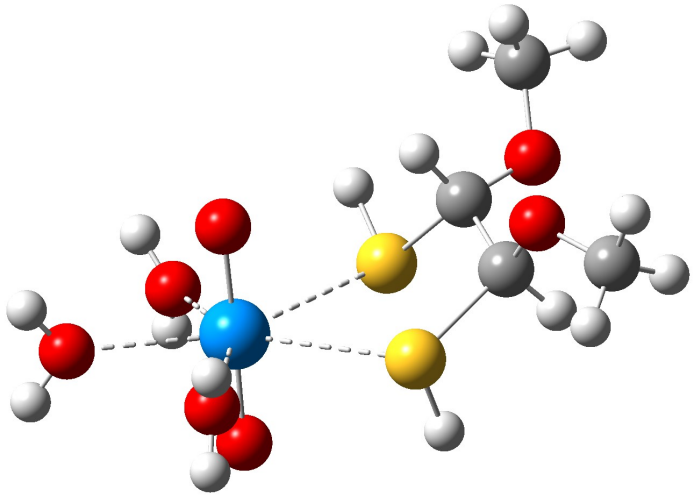

Figure 84. 1,2-Ethanedithiol with two methoxy groups in the equatorial-equatorial position (EDA-S-2-OCH3-2-EQEQ)

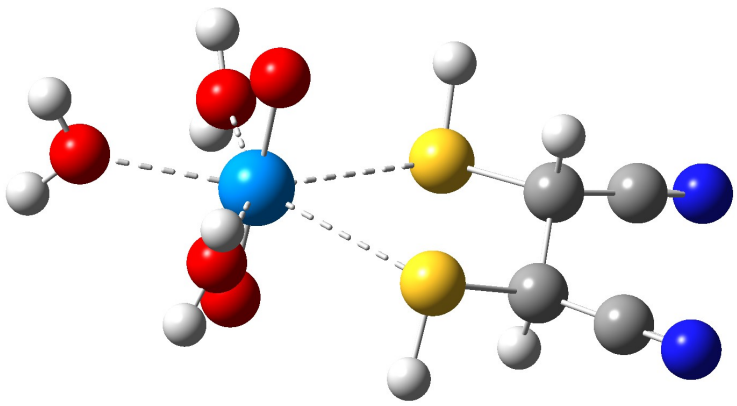

Figure 85. 1,2-Ethanedithiol with two cyanide groups in the equatorial-equatorial position (EDA-S-2-CN-2-EQEQ)

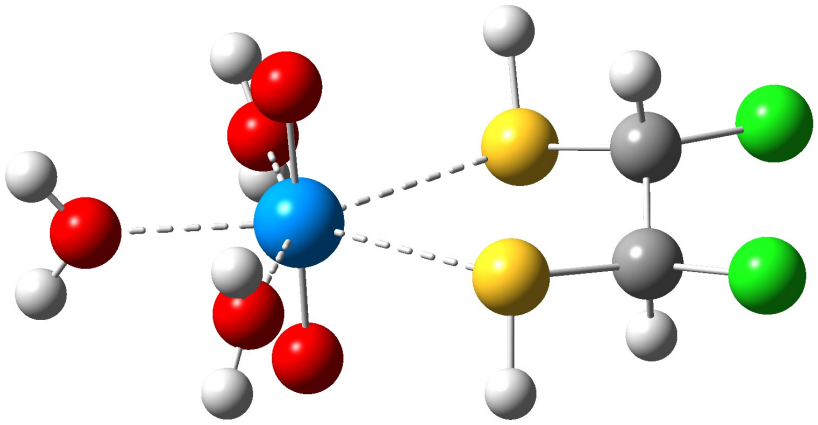

Figure 86. 1,2-Ethanedithiol with two chlorine groups in the equatorial-equatorial position (EDA-S-2-Cl-2-EQEQ)

CHAPTER FOUR: CONCLUSIONS AND FUTURE DIRECTIONS

The DFT calculations shown above investigate commonalities and differences in various nitrogen and sulfur donor uranyl complexes. The affinity and spontaneity of nitrogen ligands with strong electron-donating substituents seem to be the strongest contender for a possible uranium extraction method. These complexes consistently had the lowest reaction Gibbs free energy values, even going below the foundation molecules. After observing the substitution of one and two sulfur atoms (cysteamine and 1,2-ethanedithiol), sulfur-containing complexes drastically increase the reaction Gibbs free energy value and only indicates that staying away from larger sulfur complexes is ideal.

For future directions, we would like to observe additional substituents such as fluorine or amine. Additionally, we would like to conduct calculations in an aqueous solvent to see all these complexes would fare in a setting similar to nuclear waste. Water would be our solvent of choice, and we would test the same thermodynamic properties as we did for this experiment.

REFERENCES

[1] Roberts, D. How to drive fossil fuels out of the US economy, quickly. 2020; https://www.vox.com/energy-and-environment/21349200/climate-change-fossil-fuels-rewiring-america-electrify.

[2] U.S. Energy System Factsheet | Center for Sustainable Systems. 2019; http://css.umich.edu/factsheets/us-energy-system-factsheet.

[3] NRC: Power Reactors. https://www.nrc.gov/reactors/power.html.

[4] NRC: Backgrounder on Radioactive Waste. https://www.nrc.gov/reading-rm/doc-collections/fact-sheets/radwaste.html.

[5] Touran, N. What about the waste? https://whatisnuclear.com/waste.html.

[6] Poinssot, C.; Rostaing, C.; Greandjean, S.; Boullis, B. Recycling the Actinides, The Cornerstone of Any Sustainable Nuclear Fuel Cycles. *Procedia Chemistry* **2012**, *7*, 349–357.

[7] El-Hinnawi, E.; Essam, *International Conference on Nuclear Power and Its Fuel Cycle*.

[8] Foresman, James; Frisch, A. *Exploring Chemistry with Electronic Structure Methods (Third edition)*; 2005.

[9] Uranium Enrichment | Enrichment of uranium - World Nuclear Association. https://www.world-nuclear.org/information-library/nuclear-fuel-cycle/conversion-enrichment-and-fabrication/uranium-enrichment.aspx.

[10] Krupka, K.; Serne, R. Geochemical Factors Affecting the Behavior of Antimony, Cobalt, Europium, Technetium, and Uranium in Vadose Sediments. **2002**,

[11] EARNSHAW, N. G.; A., *Chemistry of the Elements*, 2nd ed.; 1997.

[12] Choppin, G.; Liljenzin, J. O.; Rydberg, J.; Ekberg, C. *Radiochemistry and Nuclear Chemistry: Fourth Edition*; Elsevier Inc., 2013; pp 1–858.

[13] *Experimental and Theoretical Approaches to Actinide Chemistry*; 2018.

[14] Froese Fischer, C. General Hartree-Fock program. *Computer Physics Communications* **1987**, *43*, 355–365.

[15] Ball, D. *Physical Chemistry*; Cengage, 2011.

[16] Levy, M. Universal variational functionals of electron densities, first-order density matrices, and natural spin-orbitals and solution of the v-representability problem. *Proceedings of the National Academy of Sciences of the United States of America* **1979**, *76*, 6062–6065.

[17] The Hohenberg-Kohn Theorems. http://cmt.dur.ac.uk/sjc/thesis_ppr/node12.html.

[18] Cabeza, L.; Martorell, I.; Miró, L.; Fernández, A.; Barreneche, C. In *Advances in Thermal Energy Storage Systems*; Cabeza, L. F., Ed.; Woodhead Publishing Series in Energy; Woodhead Publishing, 2015; pp 1–28.

[19] Hohenberg, P.; Kohn, W. Inhomogeneous electron gas. *Physical Review* **1964**, *136*, B864.

[20] Townsend, L. T.; Shaw, S.; Ofili, N. E. R.; Kaltsoyannis, N.; Walton, A. S.; Mosselmans, J. F. W.; Neill, T. S.; Lloyd, J. R.; Heath, S.; Hibberd, R.; Morris, K. Formation of a U(VI)–Persulfide Complex during Environmentally Relevant Sulfidation of Iron (Oxyhydr)oxides. *Environmental Science & Technology* **2019**, acs.est.9b03180.

[21] Hancock, R. D.; Bartolotti, L. J. A DFT study of the affinity of lanthanide and actinide ions for sulfur-donor and nitrogen-donor ligands in aqueous solution. *Inorganica Chimica Acta* **2013**, *396*, 101–107.

[22] Guillaumont, D. Actinide(III) and lanthanide(III) complexes with nitrogen ligands: Counterions and ligand substituent effects on the metal–ligand bond. *Journal of Molecular Structure: THEOCHEM* **2006**, *771*, 105–110.

[23] Frisch, M. J. et al. Gaussian 09 Revision E.01. Gaussian Inc. Wallingford CT 2009.

[24] Ochterski, J. W.; Ph, D. Thermochemistry in Gaussian. *Gaussian Inc Pittsburgh PA* **2000**, *264*, 1–19.

[25] Moss, G. P. Basic terminology of stereochemistry (IUPAC Recommendations 1996). *Pure and Applied Chemistry* **1996**, *68*, 2193–2222.